

The therapeutic potentials of human
neural stem cells transplantation into
the brain of the APP^{sw} (amyloid β
precursor protein swedish mutation)
transgenic mice

Ilshin Lee

Department of Medical Science
The Graduate School, Yonsei University

The therapeutic potentials of human
neural stem cells transplantation into
the brain of the APP^{sw} (amyloid β
precursor protein swedish mutation)
transgenic mice

Directed by Professor Kook In Park

Doctoral Dissertation submitted to the Department of
Medical Science, the Graduate School of Yonsei
University in partial fulfillment of the requirements for
the degree of Doctor of Philosophy of Medical Science

Ilshin Lee

December 2010

This certifies that the Doctoral
Dissertation of Ilshin Lee is approved.

Thesis Supervisor : Kook In Park

Thesis Committee Member#1 : Il Nam Sunwoo

Thesis Committee Member#2 : Joon Soo Lee

Thesis Committee Member#3 : Yong Jeong

Thesis Committee Member#4 : Chul Hoon Kim

The Graduate School
Yonsei University

December 2010

ACKNOWLEDGEMENTS

I am deeply thankful to my supervisor, Kook In Park, whose encouragement, guidance and support from the initial to the final level enabled me to develop an understanding of the doctoral dissertation.

I also thank to Il Nam Sunwoo, Joon-Soo Lee, Yong Jeong, and Chul Hoon Kim professors in helping me to broaden my view and knowledge.

I offer my regards and blessings to lab members supported me in any respect during the process of doctoral dissertation.

Lastly, I pay my respects and love to my parents, wife, and all other family members for their love and encouragement.

<TABLE OF CONTENTS>

ABSTRACT	1
I. INTRODUCTION	3
II. MATERIALS AND METHODS	7
1. Culture of human neural stem cells and preparation for transplantation	7
2. Lenti-viral vectors transduction to hNSCs or SK-N-MC cells	7
3. Naturally secreted A β oligomers derived from SK-N-MC cells -	8
4. Human NSC viability measurement	8
5. Senescence-associated β -galactosidase activity assay	9
6. In vitro differentiation studies of hNSCs	10
7. Reverse transcriptase PCR (RT-PCR)	10
8. AD-like pathological animal model	11
9. Animal surgery and transplantation of hNSCs	11
10. Tissue processing	11
11. Immunohistochemistry	12
12. Western blot and enzyme linked immunosorbent assay (ELISA)	13
13. Pro-inflammatory cytokines treatment to hNSCs in vitro	14
14. TUNEL assay for tissue	14
15. Behavioral experiment	14
16. Statistical analysis	16

III. RESULTS

1. Human neural stem cells form self-renewing neurospheres and have multipotency. ----- 18
2. Human NSCs show decrease of proliferation and differentiation into glia when cocultured with naturally secreted A β oligomers. - 22
3. Transgenic mice carrying NSE-controlled APPsw present AD-like pathology. ----- 29
4. Human NSCs engraft, migrate, and differentiate into multiple lineages in the brains of APPsw tg mice. ----- 31
5. Transplantation of hNSCs ameliorates spatial memory, motor learning, and female forelimb strength of APPsw tg mice. ----- 37
6. Transplantation of hNSCs into APPsw tg mice leads to reduction of A β 42 . ----- 43
7. Human NSC grafting suppresses the phosphorylation of endogenous tau in APPsw tg mice. ----- 48
8. Transplantation of hNSCs in APPsw tg mice attenuates astrogliosis and microgliosis. ----- 50
9. Human NSCs in the brains of APPsw tg mice increase hippocampal synaptic density and host cells survival ----- 53

IV. DISCUSSION ----- 57

V. CONCLUSION ----- 63

REFERENCES ----- 65

ABSTRACT(IN KOREAN) ----- 73

LIST OF FIGURES

Figure 1. Neurosphere formation by fetal human CNS tissue and cellular composition of the neurosphere. -----	19
Figure 2. Under differentiation conditions, hNSCs differentiate into multiple-lineages.-----	21
Figure 3. Generation of naturally secreted A β oligomers -	24
Figure 4. The proliferation of hNSCs is decreased when to expose naturally secreted A β oligomers derived from lenti-APPsw_GFP infected SK-N-MC cells -----	25
Figure 5. The conditioned media of lenti-APPsw_GFP infected SK-N-MC cells alters the fate of hNSCs --	26
Figure 6. Naturally secreted A β oligomers induce gliogenesis of hNSCs -----	27
Figure 7. APPsw tg mice show AD-like pathogenic phenotype -----	30
Figure 8. Engraftment of hNSCs transplanted into the LVs of APPsw tg mice -----	32
Figure 9. Engrafted donor-derived hNSCs differentiate into neurons, astrocytes and oligodendrocytes in the brain of APPsw tg mice -----	34
Figure 10. Differentiation of grafted hNSCs into neurons and glial cells -----	36

Figure 11. Behavioral phenotype of hNSC or H-H buffer transplanted mice	40
Figure 12. Intracerebroventricular injection of hNSCs reduces intracellular A β 42 aggregates in the hippocampi and cortexes of APPsw tg mice	45
Figure 13. The transplantation of hNSCs modulates levels of A β 42 in the brains of APPsw tg mice and hNSCs express A β degradases in vitro and in vivo	47
Figure 14. Reduction of phosphorylated tau and tau-related signal pathway in hNSC grafted APPsw tg mice ---	49
Figure 15. Analysis of astrogliosis in the brain of hNSC grafted and H-H buffer injected APPsw tg mice ----	51
Figure 16. Analysis of microglial activation in hNSC grafted and H-H buffer injected APPsw tg mice	52
Figure 17. Human NSCs augment synaptic density	55
Figure 18. Human NSCs have an anti-apoptotic effect via secretion of trophic factors in the brains of APPsw tg mice	56

LIST OF TABLES

Table 1. Sequences of primers used for RT-PCR -----	17
Table 2. Effects of hNSCs transplanted into APP ^{sw} tg mice on the elevated plus maze -----	39

ABSTRACT

Therapeutic potentials of human neural stem cells transplantation into the brain of the APPsw (amyloid β precursor protein swedish mutation) transgenic mice

Ilshin Lee

*Department of Medical Science
The Graduate School, Yonsei University*

(Directed by Professor Kook In Park)

Alzheimer's disease (AD) is an inexorable neurodegenerative disease that commonly occurs in elderly adults. AD patients exhibit memory loss and cognitive impairment. The postmortem brains of AD patients reveal abnormal accumulations of amyloid beta ($A\beta$) in the spaces around synapses and of a hyperphosphorylated form of the tau protein in the cell bodies of neurons. These $A\beta$ peptides and hyperphosphorylated tau cause synaptic dysfunction, generate neuroinflammation, disturb neuronal ionic homeostasis, and advance neuronal injury in AD.

Neural stem cells (NSCs) have the capacity for self-renewal and can give rise to differentiated neural cell types; neurons, astrocytes and oligodendrocytes. When NSCs are administrated into a diseased or injured brain, they show not only preferential extensive migration to and engraftment within areas of lesions but also the capability to replace injured cells in an appropriate manner. Apart from replacing lost cells, NSCs based therapy can provide a regenerative environment for other cells residing in diseased brains.

In the present study, we investigated the therapeutic potentials of human NSCs by using AD animal model expressing the human APP695 Swedish mutant (KM595/596NL) directed by the NSE promoter (APPsw trasgenic mice) and

APPsw-expressing SK-N-MC cells. Human NSCs (hNSCs) were isolated from human fetal telencephalon at 13 weeks of gestation and cultured as neurospheres. When naturally secreted A β oligomers derived from APPsw-expressing SK-N-MC cells were directly administered to hNSCs, cells showed the decreased proliferation and enhanced differentiation into glial cells in vitro. After the transplantation of hNSCs into the lateral ventricles (LVs) of 13-month-old APPsw transgenic mice, donor-derived cells showed the engraftment, migration and integration into the host brains. Some of transplanted cells differentiated into neurons, astrocytes and oligodendrocytes, but most of cells remained as immature cells. Human NSCs grafts effectively reduced the level of soluble A β 42 and phosphorylated tau in the cortex and hippocampus of the mice through the presence of distinct A β degradases and neurotrophins produced by implanted cells. Additionally, the administration of hNSCs had a neuroprotective effect via the secretion of trophic factors and anti-inflammatory cytokines, therefore reduced cell death and inflammation in the host brain. Finally, hNSC grafts significantly improved spatial memory and motor learning in the transgenic mice compared to the mice in which H-H buffer was injected into the brain. These findings suggest that human NSCs act through multiple potentially therapeutic actions to benefit AD mice.

Key Words : Alzheimer's disease (AD), amyloid β precursor protein (APP), amyloid β (A β), phosphorylated tau, human neural stem cells (NSCs), transplantation, cell therapy

**The therapeutic potentials of human neural stem cells transplantation
into the brain of the APP^{sw} (amyloid β precursor protein swedish
mutation) transgenic mice**

Ilshin Lee

*Department of Medical Science
The Graduate School, Yonsei University*

(Directed by Professor Kook In Park)

I. INTRODUCTION

Alzheimer's disease (AD) is a devastating neurological disorder that occurs to nearly 7 percent of the population at the age of between 65 and 74¹. The risk of AD dramatically increases in individuals beyond the age of 85 and it is predicted that incidence of AD will increase threefold within the next 50 years¹⁻³. The clinical symptoms of AD exhibit memory loss and cognitive impairment².

Microscopic examination of the postmortem brains of AD patients reveals abnormal accumulations of a small fibrillar peptide, termed an amyloid beta ($A\beta$), in the spaces around synapses (amyloid plaques)⁴ and of a hyperphosphorylated form of the tau protein in the cell bodies of neurons (neurofibrillary tangles; NFT)⁵. Most plaques and tangles appear in brain regions involved in learning and memory process⁶. The $A\beta$ peptide, which is the primary protein component of diffusible and neuritic plaque, originated through proteolytic cleavage of the amyloid precursor protein (APP) by β -secretase and γ -secretase⁷. Roughly spherical, extracellular deposits of these $A\beta$ fibrils surround dystrophic axons and dendrites activate microglia and induce astrogliosis. The exact function of the APP holoprotein is not yet established but a number of the APP mutations which cause autosomal dominant inheritable forms of

familial AD increase the production of the A β 1-42 and develop AD⁷⁻⁸. In the light of the A β cascade hypothesis, elevated A β levels or A β 42/A β 40 ratio may enhance oligomer formation, occur synaptic dysfunction, generate neuroinflammation, disturb neuronal ionic homeostasis, and advance neuronal injury⁹⁻¹¹. Under normal physiology, tau regulates the assembly and maintenance of the structural stability of microtubules, but in AD, the hyper-phosphorylated tau protein cultivates NTFs that exhibit altered soluble properties and form filamentous structures⁵. The hyper-phosphorylated tau has reduced affinity to microtubules, potentially disrupted axonal transport, therefore tau dysfunction may play a vital role in AD^{5,12}. Above all, the formation of both plaques and tangles in AD-relevant brain regions including the hippocampus, amygdala, cortex and subcortex enables one to suppose the relationship to crucial neurological process, such as learning and memory, synaptic plasticity and brain inflammation¹¹⁻¹⁴. Mutations in presenilin1 (PS1) and presenilin2 (PS2), which are polytopic membrane proteins which function as the catalytic subunit of γ -secretase, also can account for the risk factor of case of AD through enhancing APP proteolysis¹⁵⁻¹⁷. According to genetic epidemiological studies, the apolipoprotein E (apoE) gene may be another risk factor for late-onset AD¹⁸. The ϵ 4 allele increases and the ϵ 2 allele decreases the morbid risk for developing AD. Individuals carrying one or two ϵ 4 alleles develop AD at a younger age and have higher amyloid-plaque compared to individuals carrying others¹⁹. Therefore apoE4 somehow contributes to the A β deposition and the brain amyloid burden^{18,20}.

Currently, many clinical researches and trials have been progressing to ameliorate AD. In the immunotherapy, some AD patients which received intramuscular injections of an A β synthetic peptide unfortunately presented meningoencephalitis although the active vaccination could markedly reduced quantities of total A β and improved memory function in the animal model^{21,22}. Most patients administered with A β specific humanized monoclonal antibody exhibited also cerebral amyloid angiopathy related to amyloid bearing vessels²³. In pharmacotherapy for AD, there are four contents classified into cholinergic treatment, NMDA receptor antagonist, antioxidants, nonsteroidal anti-inflammatory drugs (NSAIDs)²⁴. One of the prominent systems

affecting the course of AD is the limbic system, which contains cholinergic neurons of the nucleus basalis magno cellularis(NBM)²⁵. Cholinergic neurons in the NBM are reduced in the early course of AD, and a choline acetyltransferase, the biosynthetic enzyme for acetylcholine, shows reduction of 60-90% in the cerebral cortex and the hippocampus of the AD brain^{25,26}. Concerning the cholinergic system, four acetylcholinesterase inhibitors have been approved by the U.S. Food and Drug Administration (FDA) for the AD therapy: tacrine, donepezil, rivastigmine, and galantamine²⁴. Memantine approved by FDA is utilized as AD medications acting on the glutamatergic system by blocking NMDA glutamate receptors²⁴. These drugs do not inhibit the broad pathogenic mechanism including the A β accumulation and the neurofibrillary degeneration in AD, but slightly ameliorate and impede symptoms of AD^{24,26}. A large body of data indicate that oxidative stress and the accumulation of free radical are a salient pathological feature of AD. Abnormal enrichments of Cu, Fe, Zn ions in the postmortem AD brain mediate A β toxicity and produce reactive oxygen species, hydrogen peroxide and hydroxyl radical^{14,27}. These observations led to the notion of antioxidants as a potential therapy, but antioxidant treatment divulged no or small effects on AD patients²⁴. NSAIDs may also have a protective effect through decrease of inflammation that secondarily occurs in AD brains²⁸. However, the benefit of NSAIDs reported in some researches might be due not to anti-inflammatory activity but to altered β -secretase activity^{21,29}. These findings support that a brief decrease of the inflammatory response is not necessarily beneficial in AD²¹. Until now, a outstanding performance of AD therapy have not been accomplished.

NSCs are described as cells that are derived from specific spatiotemporal neural tissues or are generated from embryonic stem cells (ESCs) and induced pluripotent stem cells (iPSCs)^{30,31}. NSCs have capacity for self-renewal and can give rise to neurons, astrocytes, and oligodendrocytes³². The stock of proliferating human NSCs (hNSCs) is mainly located in the subventricular zone (SVZ) and the subgranular zone (SGZ) of dentate gyrus in the adult brain³³⁻³⁶. Human NSCs can also be derived from developing human fetal brain between 8-20 weeks of gestation^{37,38}. These multipotent

NSCs derived from the developing or adult brain can be cultured and grown in the presence of mitogens, such as epidermal growth factor (EGF) and fibroblast growth factor-2 (FGF2) either as monolayers or as free floating spherical aggregates named the neurosphere³⁷⁻⁴⁰. When neural stem cells (NSCs) are implanted into a diseased or injured nervous system, they show not only preferential extensive migration to and engraftment within areas of discrete abnormalities but the capability to replace diseased tissue in an appropriate manner⁴¹⁻⁴⁴. Apart from replacing lost cells, NSC based therapy can also provide a regenerative microenvironment for other cells residing of diseased brains⁴⁴⁻⁴⁸.

In this point of view, NSC grafting has a possibility to improve deficits of AD although the widespread and progressive pathology still offer an extremely problematic situation in AD. Recently, hNSCs transplanted into aged rodent brains differentiated into each neural cells and significantly improved the cognitive functions of the animals^{48,49}. Mouse NSCs grafted into hippocampi of an AD animal model also exhibited a upregulation of hippocampal synaptic density and improved cognition. These reports indicate that hNSCs may be promising candidate for AD therapy⁴⁸⁻⁵².

In this study, we examine whether in the AD animal model, hNSCs transplantation can alter AD-like pathology, especially cognitive function.

II. MATERIALS AND METHODS

1. Culture of human neural stem cells and preparation for transplantation

Human fetal tissue aborted at 13 weeks of gestation was provided with full patient consent and the approval of the research ethics committee of Yonsei University College of Medicine⁵³. The methods of acquisition conformed to NIH and Korean Government guidelines. Human NSCs were isolated from fetal telencephalic brain tissues by chopping and trypsinization, and seeded into tissue culture-treated 100-mm plates (Corning Incorporated Life Science, Lowell, MA, USA) at a density of 200,000 cells/ml of serum-free growth medium, which consisted of a 1:1 mixture of Dulbecco's modified Eagle's medium and Ham's F12 (DMEM/F12; Gibco, Carlsbad, CA, USA) supplemented with penicillin/streptomycin (1% vol/vol; Gibco) and N2 formulation (1% vol/vol; Gibco). Mitogenic stimulation was achieved by adding 20 ng/ml fibroblast growth factor-2 (FGF-2; R&D Systems Inc, Minneapolis, MN, USA) and 10 ng/ml leukemia inhibitory factor (LIF; Sigma-Aldrich Corp, St. Louis, MO, USA). Heparin (8 $\mu\text{g}/\text{ml}$; Sigma-Aldrich Corp) was added to stabilize FGF-2 activity. All of the cultures were maintained in a humidified incubator at 37°C and 5% CO₂ in air, and half of the growth medium was replenished every 3-4 days. Cells from each region of the human CNS tissue formed neurospheres during the first 2-5 days of growth. Passaging was undertaken every 7-8 days by dissociation of bulk neurospheres with 0.05% trypsin/EDTA (T/E; Gibco). The neurospheres were re-seeded into fresh growth medium at a density equivalent to approximately 200,000 cells/ml. Transplanting to the brain of mice, proliferating hNSCs were labeled by the 5-Bromo-2-deoxyuridine (BrdU; Sigma-Aldrich Corp) administration into culture medium for 5 days and then were dissociated to single cells using 0.05% trypsin/EDTA. Dissociated cells were subsequently washed 3 times with H-H buffer (1×Hank's balanced salt solution, 10mM HEPES, pH 7.4; Gibco) and were diluted in the appropriate volume of H-H buffer to obtain a suspension of 1×10^5 cells/ μl .

2. Lenti-viral vector transduction to hNSCs or SK-N-MC cells

The following lenti-vectors were used: human APP695 Swedish mutant (K595N/M596L)⁵⁴-eGFP or only eGFP. All recombinant lenti-viruses were produced using

transient transfection into 293T cells. Subconfluent 293T cells were co-transfected with 20 μ g pWPI transfer vector containing interest gene, 15 μ g psPAX2 packaging construct, and 6 μ g pMD2G envelop plasmid by calcium phosphate precipitation. The lenti viral vectors were donated from Trono lab. After 3 hours, the media was changed with fresh medium, recombinant lentiviruses were harvested 48 hours later, and viruses were concentrated by ultracentrifugation under the sucrose cushion. The viral titer was checked as transducing unit (TU) via flow cytometry method offered by Trono lab (<http://tronolab.epfl.ch/>). To transduce recombinant lenti-viruses, hNSCs were seeded onto cell culture dishes with serum-free growth medium containing FGF2, LIF, and heparin, and SK-N-MC cells were seeded in serum free growth medium without mitogen. One hour later, lenti-viral particles encoding eGFP or APPsw-eGFP were respectively added to well with a multiplicity of infection (MOI) of one. The media was replaced with fresh one the next day, and each cells transduced with lenti-viral vector were cultured over 1 month to confirm the stable expression of interest gene.

3. Naturally secreted A β oligomers derived from SK-N-MC cells

Naturally secreted cell-derived human A β was obtained from culture media of SK-N-MC cells stably expressing human APP695, containing the K595N/M596L Swedish mutation. SK-N-MC cells transduced or untransduced with lenti-APPsw_GFP were cultured in N2 media. The cells were seeded with plain N2 media and then incubated in this media (10ml/10cm dish) for 3 days. At the end of this period, medium were harvested and cleared by centrifugation at 750g for 5 minutes. The conditioned media made aliquots for next experiment and the presence of monomeric and oligomeric A β was assessed by immunoprecipitation and western blotting.

4. Human NSCs viability measurement

Human NSCs were cultured into 12 well culture dishes at approximately 5×10^5 cells/well without mitogen for 24 hours to arrest the cell cycles, and next were daily changed with conditioned medium derived from SK-N-MC cells transduced or untransduced with lenti-viral vector for 3days. Cell viability was assessed using Cell Counting Kit-8 (CCK 8; Dojingo Molecular Technologies, Inc, Rockville, MD, USA)

containing WST-8 (2-(2-methoxy-4-nitrophenyl)-3-(4-nitrophenyl)-5-(2,4-disulfophenyl)-2H-tetrazolium, monosodium salt), which is reduced by dehydrogenases in cells to give a yellow-colored product, formazan. The amount of the formazan dye generated by the activity of dehydrogenases in cells is directly proportional to the number of living cells, thus allowing estimation of the number of viable cells in the medium by absorbance at 450nm. Human NSCs proliferation was determined by quantifying DNA replication using BrdU, a thymidine analogue, which enables the detection of actively proliferating cells that have progressed in S phase. Cells were seeded onto 6 well culture dishes at approximately 1×10^6 cells/well without mitogen for 24 hours to stop the cell cycles. Cells next were incubated with BrdU at a final concentration of 3 μ M for 3 days changing the medium with conditioned medium daily, and were then fixed with a 100% ethanol. After cell membrane permeabilization using 2N HCl, the cells were labeled with an anti-BrdU antibody (Sigma-Aldrich Corp) and FITC conjugated anti-mouse IgG secondary antibody (Vector Laboratories, Inc, Burlingame, CA, USA). Cells next were counted by flow cytometry analysis. Terminal dUTP nick end labeling (TUNEL) assay was performed using *In Situ* Cell Death Detection Kit (Roche Applied Science, Indianapolis, IN, USA). Cells were fixed with 4% paraformaldehyde (PFA) in PBS for 1hour at room temperature. The samples were washed with PBS and then permeabilized by 0.1% Triton X-100 in 0.1% sodium citrate buffer for 15 minutes at 4 $^{\circ}$ C. After 3 times washing, cells were resuspended in TUNEL reaction mixture (Roche Applied Science), and incubated for 60 minutes at 37 $^{\circ}$ C. TUNEL positive cells were quantified by flow cytometry.

5. Senescence-associated β -galactosidase activity assay

Equal numbers of hNSCs, which are treated with conditioned medium of lentiviral APPsw transduced SK-N-MC cells or untransduced SK-N-MC cells, were collected, washed and resuspended in either 0.1M citrate buffer (pH 4.5) or 0.1M phosphate buffer (pH 6.0). Cells were lysed by freezing and thawing. The cell lysates were centrifuged at 12000g for 7 minutes. The supernatant was mixed with Chlorophenol red- β -D-galactopyranoside (CPRG 2.2 μ g/ μ l; Sigma-Aldrich Corp) and 10mM MgCl₂. Heat inactivation control was prepared for 3minutes at 65 $^{\circ}$ C. After incubation at 37 $^{\circ}$ C for over night, 1.5 volumes of 1M Na₂CO₃ were added to stop the reaction and absorbance at 570nm was measured.

6. In vitro differentiation studies of hNSCs

Whole neurospheres originated from the hNSC were dissociated into a single cell suspension in T/E and directly plated onto poly-L-lysine (PLL, $10\mu\text{g}/\text{mL}$; Sigma-Aldrich Corp) coated 8-well chamber slides (Nunc, Rochester, NY, USA) in DMEM/F-12 that contained N2 supplement but without mitogens. Over the 7 days period following plating, the cells formed a differentiating neuronal and glial monolayer. The cells were fixed on 7 days with 4% PFA in 0.1M PIPES buffer (pH 6.9) for 10 minutes, rinsed three times with phosphate-buffered saline (PBS), and treated as described below. The fixed cells were blocked with 3% bovine serum albumin (BSA) and 10% normal horse serum (Vector Laboratories, Inc) with 0.01% or 0.2% Triton X-100 and incubated with primary antibodies; human nestin (1:200; Millipore, Billerica, MA, USA), GFAP (1:1000; DAKO, Glostrup, Denmark), β -tubulin III (Tuj1, 1:1000; Covance, Princeton, NJ, USA), NF H, M, and L (neurofilament HML, 1:1000; Millipore), O4 (1:30; Millipore), APC-CC1 (1:30; abcam, Cambridge, UK), Glutamin synthetase (GS, 1:1000; Sigma-Aldrich Corp), S100 β (1:1000; Sigma-Aldrich Corp), Galactocerebroside (GalC, 1:100; Sigma-Aldrich Corp), PDGFR- α (1:100; Santa Cruz Biotechnology, inc, Santa Cruz, CA, USA). Following rinsing with PBS, the slides were incubated with species-specific secondary antibodies conjugated with fluorescein or Texas Red (1:200; Vector Laboratories, Inc). 4',6'-diamidino-2-phenylindole (DAPI; Vector Laboratories, Inc) was used as the nuclear stain. After immunofluorescence staining, the percentage of immunoreactive cells was calculated using a fluorescence microscope (Olympus, Tokyo, Japan). For each group, the cells of 10 fields that included 100-500 cells were counted. The number of total cells was evaluated by counting DAPI-positive nuclei.

7. Reverse transcriptase PCR (RT-PCR)

Total RNA was prepared from hNSCs treated with conditioned medium in vitro or mice brain tissue 7 weeks after transplantation respectively using TRI Reagent (Molecular Research Center, Inc, Cincinnati, OH, USA). RNAs were quantified spectrophotometrically, and then $5\mu\text{g}$ of isolated RNA was reverse transcribed using SuperScriptTM III Reverse Transcriptase (Invitrogen, Carlsbad, CA, USA) in $20\mu\text{l}$ reaction volume for cDNA synthesis. Thereafter, $1\mu\text{l}$ cDNA was used for PCR in 20

μl volume. Primers were used to detect expression of lineage specific markers, human A β degradases, human growth factors, and human anti inflammatory cytokines (Table 1). PCR products were confirmed with 1.5% agarose gel electrophoresis and staining of ethidium bromide.

8. AD like-pathological animal model

APP Swedish transgenic (APP^{sw} tg) mice expressed the human APP695 Swedish mutant which is controlled by the neuron specific enolase (NSE) promoter⁵⁵. Male transgenic mice were bred with background matched wild type female mice, C57BL/6. Founder APP^{sw} tg mice were kindly endowed from Korea Food & Drug Administration (KFDA), Nat'I Inst. Toxicol. Res. To determine whether any mouse has the human APP695 Swedish mutant, a genotyping carried out at 3-4 weeks using PCR of genomic DNA isolated from mice tails. As the primer of PCR, sense primer used 5'-TCTAGATCGCGATGCTGC-3' and anti-sense primer used 5'-GTCTAGAGTC-TAGTTCTGCATC-3'. Same litters were randomly selected for the experimental or control groups.

9. Animal surgery and transplantation of hNSCs

13month-old APP^{sw} mice or aged matched wild mice were fully anesthetized using a mixture of ketamine and xylazine to execute stereotactic implantation of hNSCs. Bilateral stereotactic injections of 5 μl hNSC suspensions were placed with a Hamilton syringe into LVs (A/P, -0.1mm from bregma; L, \pm 0.9mm; D/V, -2.0mm from dura mater). Injection speed was 1 $\mu\text{l}/\text{min}$ and the needle was kept in place for additional 2.5 minutes before it was slowly withdrawn. The surgical area was cleaned with sterile saline, and the incision was sutured. As a control, mice received 5 μl H-H buffer at the same method.

10. Tissue processing

After hNSC or H-H buffer implanting mice were followed up until 7 weeks, they deeply slept with anesthetic cocktail. They were then transcardially perfused with cold PBS followed by cold 4% PFA in 0.1M PIPES solution. The brain carefully

extracted, fixed for overnight in 4% PFA in 0.1M PIPES solution at 4°C, and subsequently transferred to 30% sucrose solution at 4°C until embedding. Optimal cutting temperature (OCT) compound was used to embed the brains and sections were cut to 18 μ m on a freezing cryostat and stored at -20°C.

11. Immunohistochemistry

Sections were briefly washed two times with PBS. For fluorescence immunohistochemistry, sections were firstly blocked with 10% normal donkey serum (Jackson ImmunoResearch Laboratories, Inc, West Grove, PA, USA) and 3% BSA in PBS adding 0.1-0.3% Triton X-100. BrdU antibody requires a pre-treatment step as following 30minutes in 2N HCl at 37°C. Primary antibodies were incubated overnight at 4°C. Appropriated secondary antibodies were applied for 1hour 10minutes at 37°C followed by 3times PBS washes, and mounted. Primary antibodies included anti-BrdU-fluorescein (1:20; Roche Applied Science), human nuclei (hNuC, 1:100; Millipore), human nuclear matrix (hNuMA, 1:25; Calbiochem, Darmstadt, Germany), GFP (1:200; Invitrogen) for tracing hNSCs, and anti-human nestin, Tuj1, Doublecortin (DCX, 1:200; Santa Cruz Biotechnology, inc), NF L,M,H, GFAP, PDGFR- α , Olig2 (1:500; Millipore) for differentiation pattern of hNSCs, and anti-CD11b (1:50; AbD serotec, Kidlington, UK), F4/80 (1:50; AbD serotec), Iba1 (1:250; Wako, Tokyo, Japan) for the microglial staining. Secondary antibodies conjugate Fluorescein, Texas Red (Jackson ImmunoResearch Laboratories, Inc). Immuno-labelling cells were observed and measured using a fluorescence microscope (Olympus) and Zeiss LSM 700 confocal microscope (Carl Zeiss, Oberkochen, Germany). For immunoperoxidase staining, sections were incubated with 0.3% H₂O₂ in methanol for blocking endogenous peroxidase activity. A β 42 immunolabelling require incubation in 90% formic acid for 7min to expose the epitope. The primary antibody was respectively applied for overnight at 4°C. Sections were developed with diaminobenzidine (DAB; Sigma-Aldrich Corp) substrate using VECTASTAIN Elite ABC kit (Vector Laboratories, Inc). The primary antibodies used anti-A β 42 (1:100; invitrogen), APP (Y188, 1:500; abcam), phosphorylated tau (AT180, 1:200; Thermo Fisher Scientific Inc, Waltham, MA, USA) for AD-like pathology.

12. Western blot and enzyme linked immunosorbent assay (ELISA)

Lysates of naive and lenti-APPsw_GFP infected SK-N-MC cells were prepared using homogenization in Tissue Protein Extraction Reagent (T-PER; Thermo Fisher Scientific Inc) supplemented with protease inhibitors (Sigma-Aldrich Corp). For immunoprecipitation of conditioned medium, Dynabeads® ProteinG (Invitrogen) 20 μ l were incubated with 2 μ g monoclonal anti-A β (6E10; Covance) in 0.01% tween20 in PBS at room temperature for 30 minutes. Both conditioned medium were added to antibody coated Dynabeads and incubated at 4°C overnight. Eluted proteins were investigated by western blot analysis.

After mice implanted with hNSCs or H-H buffer followed up until 7 weeks, the brains of mice were homogenized in T-PER supplemented with protease inhibitors and phosphatase inhibitors (Sigma-Aldrich Corp). The homogenized mixes were briefly sonicated to shear the DNA and centrifuged at 4°C for 1 hour at 100,000g. The supernatant was stored as the soluble fraction. The pellet was re-homogenized in 70% formic acid and centrifuged at 4°C for 1 hour at 100,000g. The supernatant was stored the insoluble fraction. Protein concentration was determined using the Bio-Rad Protein Assay (Bio-Rad, Hercules, CA, USA) based on Bradford assay. Proteins were resolved by SDS/PAGE under reducing conditions and transferred to nitrocellulose membrane. The membrane was incubated in a 5% nonfat milk in TBS containing 0.1% tween20 (TBST) for 1 hour. After overnight incubation at 4°C with the APP, human APP (abcam), 6E10, tau (Sigma-Aldrich Corp), phosphorylated tau (Cell Signaling Technology (CST), Danvers, MA, USA), AT180, TrkA/B (CST), phosphorylated TrkA/B (CST), Akt (CST), phosphorylated Akt (CST), GSK3 β (Santa Cruz Biotechnology, inc), phosphorylated GSK3 β (CST), CREB (CST), phosphorylated CREB (CST), BDNF (Santa Cruz Biotechnology, inc), active caspase3 (BD Bioscience, Franklin Lakes, NJ, USA) antibodies, the membrane was washed in TBST for 20 minutes and incubated at room temperature with peroxidase conjugated anti mouse or rabbit antibodies (Jackson ImmunoResearch Laboratories, Inc) for 1 hour. The blot was washed in TBST for 20 minutes, slightly treated with SuperSignal West Pico Chemiluminescent Substrate (Thermo Fisher Scientific Inc), and interesting bands were sensitively detected using LAS 4000 mini (GE Healthcare, Buckinghamshire, UK). ELISA measurements of A β 42 and A β 40 were conducted using the human A β 1-42 or A β 1-40 assay kit (Immuno-Biological Laboratories Co., Gunma, JAPAN) in

accordance with the manufacturer's instructions after soluble fraction was diluted with TBS pH7.4 and insoluble fraction was diluted with TBS pH10.6.

13. Pro-inflammatory cytokines treatment to hNSCs in vitro

Human NSCs were treated with IFN γ 50ng/ml (PeproTech, Rocky Hill, NJ, USA), TNF α 20ng/ml (PeproTech), and IL1 β 10ng/ml (R&D Systems Inc) for 24 or 48 hours. For this experiment, cells were seeded 8×10^5 cells/well on 6well culture dish with mitogen as proliferation condition, and cells were seeded 1.2×10^6 cells/well on PLL coated 6well culture dishes without mitogen as differentiation condition. After 3 days, proliferating hNSCs were exposed to cytokines. Differentiating hNSCs were maintained for 5days and followed to exposure of cytokines. The cells were processed for RT-PCR

14. TUNEL assay for tissue

The fixed cryopreserved brain sections on a slide were blocked endogenous peroxidase with 3% H₂O₂ in methanol for 10min, permeabilized with 0.1% Triton X100 in 0.1% sodium citrate buffer prepared freshly, and blocked with 10% normal donkey serum in PBS for 30 minutes. The sections were then incubated with *In Situ* Cell Death Detection Kit (Roche Applied Science) following the manufacturer's procedures. Negative controls were only treated with Label Solution instead of the TUNEL reaction mixture. Positive controls were incubated with DNase I (Roche Applied Science) to induce DNA strand breaks and labeled with the TUNEL reaction mixture. Incubation was performed in a humidified chamber for 1 hour at 37°C. The sections were labeled with Converter-POD for 30 minutes at 37°C, and then developed with DAB substrate. The slides were analyzed using a microscope. Normal nuclei, which contained only insignificant amount of DNA3'-OH ends, did not stain with this technique, however, cells with apoptotic morphology exhibited condensed nuclei labeling.

15. Behavioral experiment

Every behavioral test perform 5 weeks after hNSC grafting.

Locomotor activity was measured in the chamber, made of white acrylic with a

50×50_{cm} surface area and with 30_{cm} transparent walls. The floor is divided by each detectors into regular 289 squares. Mice were placed in the center of the chamber for 1 hour per session for 24 hours. The number of ambulatory and stereotyped activity were recorded by infrared beam break detection system. Stereotyped movements were recorded whenever the mice sway from one side to the other or else engage in scratching or grooming movements.

Open field test was measured in the same chamber under strong light illuminating. A mouse was placed at the center of the chamber floor, and allowed to freely explore recording for 5 minutes per session for 30 minutes with the same apparatus. On each experiment finishing, the number of feces was counted.

Accelerating rotarod test consisted of a beam made of knurled white plastic (diameter: 3_{cm}, width: 6_{cm}), which provides a firm grip. The rotarod gradually accelerated from 4 to 40 rpm over the 5 minutes test period. Latencies before falling were measured for three trials.

Wire maneuver test consisted of a horizontal steel wire (diameter: 2_{mm}, length: 55_{cm}) flanked by two side bars. The wire was placed at a height of 52_{cm} from the cushioned floor. Mice were placed upside-down in the middle of the horizontal wire. The test was performed until falling for 3 minutes.

Elevated plus maze was made of black plastic, consisting of four arms (length: 60_{cm}, width: 5_{cm}, height from floor: 40_{cm}) in a cross shaped form and a central region (5×5_{cm}). Two of the arms are enclosed on three sides by walls (height: 16_{cm}), whereas the other two are not. The two enclosed arms face each other, and the two open arms face each other as well. Mice were firstly placed in the center region and their behavior evaluated for 5 minutes. The number of entries (four paw criterion) and the time spent in either the enclosed or the open arms was measured, together with the open/total number of entries and duration ratios. The open arm duration began once the mice first entered either open arm from the central region and was accumulated until entry into either enclosed arm. Conversely, enclosed arm duration was accumulated until entry into either open arm.

Morris water maze was evaluated in basin (diameter: 90_{cm}, height of the wall: 30_{cm}), filled skim milk solution at 22°C to the height of 20_{cm}. Mice were placed next to and facing the wall successively in north, east, south, and west positions, with the escape platform hidden 1_{cm} beneath water level in the middle of the northwest quadrant. The swimming trajectory was monitored by the video tracking system. The

pool was separated into four equally spaced quadrants. The number of quadrant entries indicating swim path length and the escape latencies were measured for four trials per session for 6 days. Whenever the mouse failed to reach the escape platform within the maximally allowed time of 60 seconds, it was manually placed on the platform for 30 seconds. The day after the acquisition phase, a probe test was conducted by removing the platform and placing the mouse next to and facing the southeast side. The time spent in the previously correct quadrant and firstly reaching to the platform region were measured during a single 60 seconds trial.

16. Statistical analysis

Statistical analyses were conducted with StatView (SAS Institute Inc., Cary, NC, USA) or SPSS (IBM Company, Somers, NY, USA). On parametric analysis, differences among multiple means with one variable were calculated by one-way ANOVA and the Dunnett or Scheffe post hoc test, and differences between two means were estimated with unpaired t-test. On non-parametric analysis, differences among multiple means with one variable were evaluated by Kruskal Wallis, and differences between two means were assessed with Mann-Whitney test. Only values with $p < 0.05$ were accepted as significant.

Table 1. Sequences of primers used for RT-PCR

Category	Gene name	Forward primers	Reverse primers
Identification	APP	GAAGCCGATGATGACGAGGA	CTCAAGCCTCTCTTTGGCTTTCTG
	β -actin	ACTGCCGCATCCTTTCCTCC	GGAGCCACCGATCCACACAGA
	GAPDH	ACCACAGTCCATGCCATCAC	TCCACCACCCTGTTGCTGTA
Cell fate	Nestin	TGGAGTCTGTGGAAGTGAACC	CATTTTCCACTCCAGCCATCC
	Tuj1	AGAGCCATCTAGCTACTGACAC	CCGAATATAAACACAACCCAGTA
	SCG10	CATCAACATCTATACTTACG	GCCAATTGTTTCAGCACCTG
	GFAP	ACATCGAGATCGCCACCTAC	ACATCACATCCTTGTGCTCC
	S100 β	GGTGGCCCTCATCGACGTTTT	TCGCCGTCTCCATCATTGTCC
	ID 1	TGCGTGTCTGTCTGAGCAGA	CTGATCTCGCCGTTGAGGGTG
	ID 3	GCTGAGCTTGCTGGACGACAT	GCTGTAGGATTTCACCTGGC
	GS	TGGGCACCCCTTGGTTGGC	CCGCATGGCCTTGGTGCTGA
	STAT3	TGCAGCAAAAAGTTTCCTACA	CAGAATGTAAATTTCCGGGA
	NG2	ACTTTGCCACTGAGCCTTAGAAT	GTTTTCGGAGGTAGAAGAGCAG
	Olig2	TTCCCTGCGACGACTATCCTCCC	GCGGCTGTGATCTTGAGACGC
	$A\beta$ degradases	IDE	TACCGGCTAGCGTGGCTTCT
MME		TTTAAGGAGCAATCCCAGTGC	CCTGGACTGTGCACATCTGTT
MMEL		ACACACGAGTGAACCTACCGCA	CCTCCAGGATGTAGTCAGGGT
ECE1		AAGGCCGATGCCATCTACAAC	TTAAGGCCCTGGGTGAGGAG
ECE2		CAGACCTGCATCTCCAACACG	GCTGGTCAGCCATAACCTTGG
MMP2		CCTTCACTTCTCTGGGCAACA	AAGGTCAATGTCAGGAGAGGC
MMP3		CAGCCAAGTGTATCCTGCTT	CGATTTTCTCACGGTTGGAG
MMP9		AAGGATGGGAAGTACTGGCGA	AAGACGTCGTGCGTGCCAAA
PLAT		CCACTGCTTCCAGGAGAGGTT	AGGAGACAAGGCCTCATGCTT
PLAU		TCTGTACCTACGTGTGTGGA	ATACATCGAGGGCAGGCAGAT
ACE		GATGGACACCACAGAGGCTAT	AAGGCCACAGGTAAGTCTTTG
CTSB		CTCTGCTGCCTGCTGGTGTT	CGGTCAGAGATGGCTTCCAC
Anti inflammatory cytokines	IL4	AAGGAAACCTTCTGCAGGGCT	CGTACTCTGGTTGGCTTCCTT
	IL1RN	AGATGTGGTACCCATTGAGCC	AATTTGGTGACCATGACGCCT
	IL10	ACAGCTCAGCACTGCTCTGTT	TGGGTCTTGGTTCTCAGCTTG
	TGF β	ATCCACCTGCAAGACTATCGA	CGGAGCTCTGATGTGTTGAAG
Neuro-trophic & growth factors	BDNF	AACAATAAGGACGCAGACTT	TGCAGTCTTTTTGTCTGCCG
	FGF2	GTGTGCTAACCGTACCTGGC	CTGGTGATTTCTTGACCGG
	GDNF	CTGACTTGGGTCTGGGCTATG	TTGTCACTCACCAGCCTTCTATT
	NT3	TACGCGGAGCATAAGAGTCAC	GGCACACACAGGACGTGTC
	NT4/5	CCTCCCCATCCTCCTTTTT	ACTCGCTGGTGCAGTTTCGCT
	VEGF	CCATGGCAGAAGGAGGAGG	ATTGGATGGCAGTAGCTGCG
	IGF-1	CAACAAGCCACAGGGTATGG	GCACTCCTCTACTTGCGTTC
NGF	ATGTCCATGTTGTTCTACACT	AAGTCCAGATCCTGAGTGTCT	

III. RESULTS

1. Human neural stem cells form self-renewing neurospheres and have multipotency

Proliferating single cells isolated from the telencephalon of human fetus at 13 weeks of gestation (termed hNSCs) give rise to free-floating spheres called neurospheres; these were identified by their phase-bright appearance (Fig. 1A)⁵³. To analyze the cellular composition of the neurospheres, we investigated the expression of lineage-specific markers. Immature cells were identified with nestin such as the NSC and radial glial marker, and radial glia were recognized by the immunolabeling of vimentin, GFAP, Pax6, and astrocyte specific transporter (GLAST or EAAT1). In addition, GFAP was used as an astrocytic marker, and Tuj1, NF, and NeuN were used as neuronal markers. These neurospheres are known to contain different subtypes of cells that express more than one of the cell fate specific proteins. Most hNSCs (95-99%) expressed vimentin, nestin, GFAP, and Pax6 (Fig. 1B, D, E, H or J), whereas GLAST positive cells were distributed in the outer regions of the sphere (Fig. 1M, N, O). More than 90% of cells that had GFAP immunoreactivity concurrently expressed nestin, vimentin, or Pax6, which suggests that they characterize radial glial cells, which are recognized as multipotent NSCs (Fig. 1B, D, E, F, J, K, L). Besides, more than 90% of cells labeled with the GFAP antibody expressed the early neuronal marker, Tuj1 in relatively low to moderate levels (Fig. 1G, H, I). These data suggest that cells double labeled with glial and neuronal markers are multipotent progenitors. Some cells that strongly expressed Tuj1 were predominantly found in the sphere core and were not colabeled with GFAP antibodies (Fig. 1H, I), suggesting that even under proliferative conditions, some early neurons are generated in the sphere. However, cells in the spheres did not express other mature neuronal markers, such as NF (Fig. 1C) or NeuN. These results demonstrate that multipotent NSCs, progenitors and radial glial cells may co-exist with some restricted neuronal or glial progenitors in human neurospheres that are derived from the fetal telencephalon^{30,35,37,53}. When plated on PLL coated dishes without mitogen, hNSCs expressed Tuj1 as a neuronal marker, GFAP as an astrocytic marker, and O4 as an oligodendrocytic marker (Fig. 2C, D, E). In addition, many hNSCs still generated nestin under this condition (Fig. 2B). These observations confirm that hNSCs are multipotent under differentiation conditions^{30,37,53}.

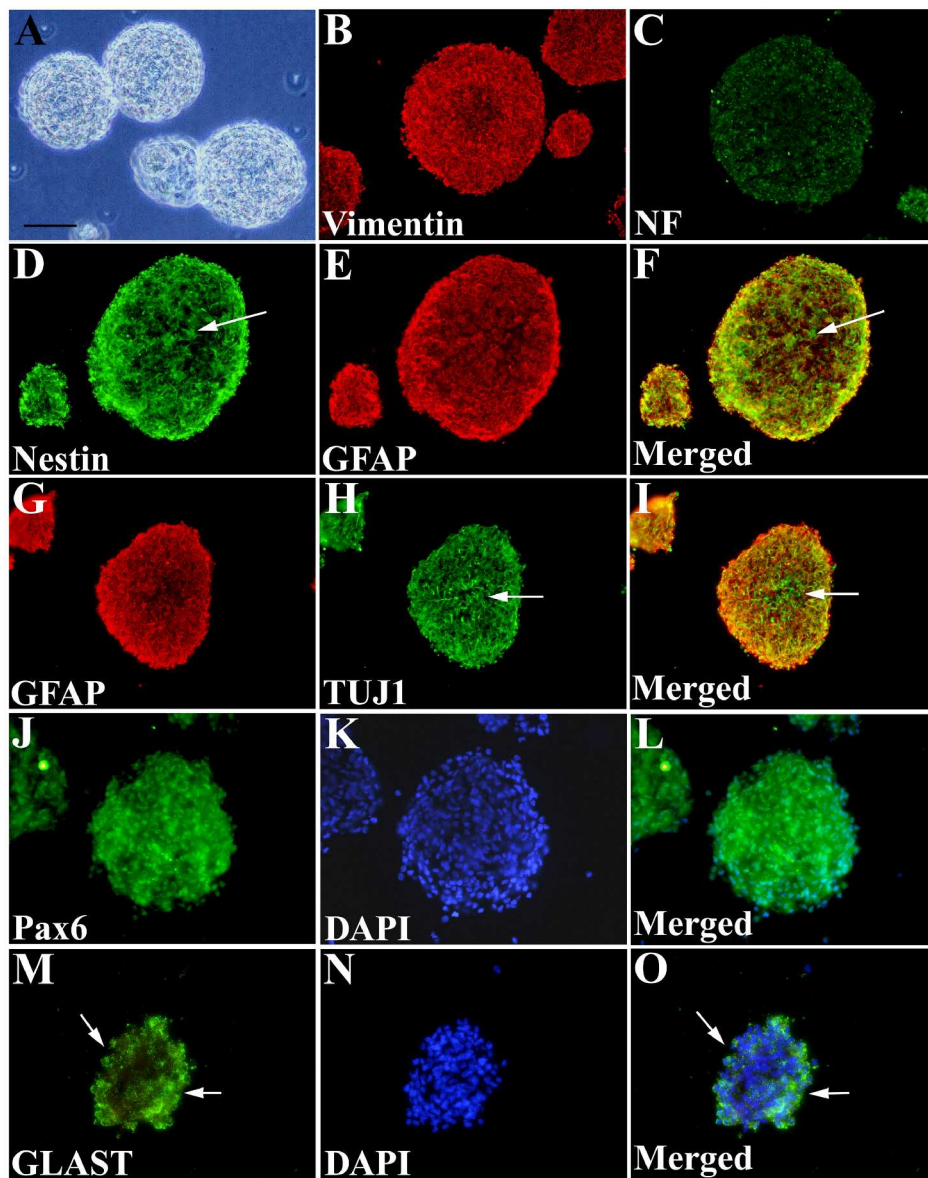


Figure 1. Neurosphere formation by fetal human CNS tissue and cellular composition of the neurosphere. Phase microscopy (A) and immunofluorescence labeling (B–O) of representative telencephalic neurospheres grown in bFGF and LIF. The sectioned neurospheres were stained for vimentin (B), NF HML(C), nestin (D and F; green), GFAP (E, G and I; red), Tuj1 (H and I; green), Pax6 (J and L; green), GLAST (M and O; green), and DAPI (K, L, N, and O; blue). Note that the majority of the cells

in the neurospheres express vimentin, nestin, GFAP, Tuj1, and Pax6 (B, D, E, H, and J, respectively), while GLAST staining appears in the outer portions of the spheres (arrows in M and O). (D–F) More than 90% of the GFAP-expressing cells (E; red) co-express nestin (D; green), as observed under the dual-filter microscope (F; yellow or orange). A few cells within the neurospheres are labeled with the anti-nestin antibody and not with the anti-GFAP antibody (arrows in D and F; green). (G–I) More than 90% of the GFAP-expressing cells (G; red) co-express Tuj1 in relatively low to moderate levels (H; green), as observed under the dual-filter microscope (I; yellow or orange). Some cells that express tuj1 at high levels, but that are not labeled with the anti-GFAP antibody, are located predominantly in the neurosphere core (arrows in H and I; green). Scale bar=100 μ m.

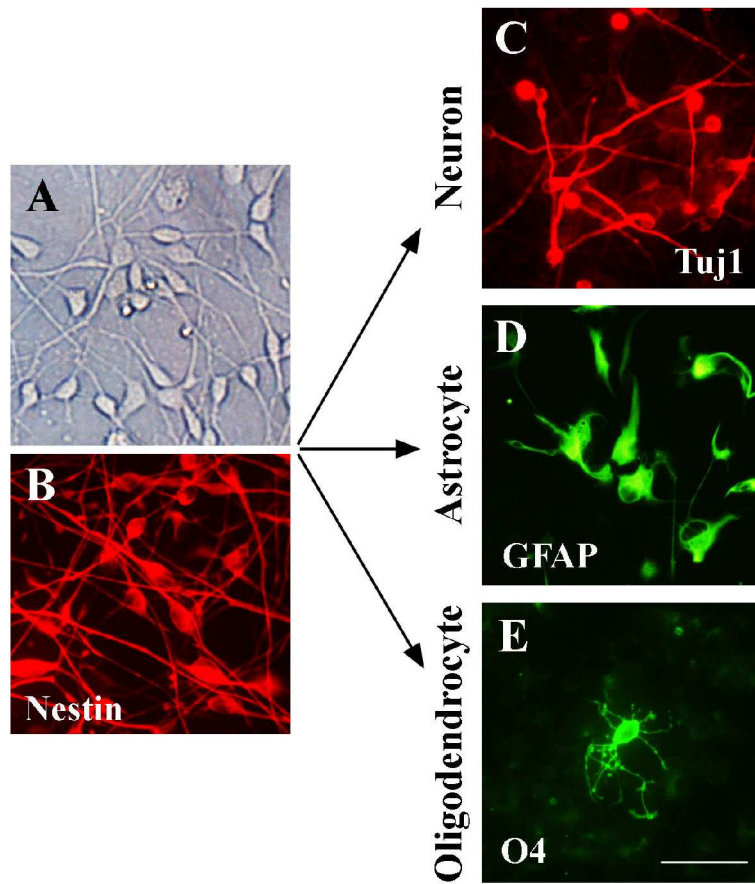


Figure 2. Under differentiation conditions, hNSCs differentiate into multi-lineages. (A) hNSCs on PLL coated culture dishes adhered the bottom of the plates, and extended process using the bright field microscope. (B) Many hNSCs still remained immature state (nestin, red). (C, D) Neuronal (Tuj1, red) and astrocytic (GFAP, green) markers were shown. (E) A few hNSCs expressed oligodendrocytic markers (O4, green). Scale bars=50 μ m.

2. Human NSCs show decrease of proliferation and differentiation into glia when cocultured with naturally secreted A β oligomers.

As a pathophysiological factor of AD, naturally secreted A β oligomers derived from APP expressing cells can inhibit hippocampal LTP and disrupt cognitive function in animal models^{11,56-58}. In previous studies, soluble oligomeric A β was detected in the conditioned media of APP expressing cells and in extracts isolated from the brains of AD patients^{59,60}. To investigate the effect of naturally secreted A β on hNSCs in vitro, SK-N-MC cells were infected with lenti-viral particles encoding the human APP695 Swedish mutation (LysMet595/596AsnLeu) and eGFP (Fig. 3A). The cells transduced with these lentiviral vectors were 60% GFP positive upon representative fluorescence-activated cell sorting analysis and abundantly encoded the *APP* gene upon PCR (Fig. 3B, C). We also confirmed higher APP and A β levels from lysates of cells infected with lenti-APPsw_GFP relative to uninfected cells. (Fig. 3D). To obtain the A β oligomers, we prepared conditioned media of untransduced cells or lenti-APPsw_GFP transduced cells at the third day after seeding. To estimate the apparent molecular weight of each A β species in each condition medium, the precipitants with the 6E10 antibody was subjected to SDS-PAGE. It has reported that A β species present monomer (4kDa), dimer (8kDa), trimer (12kDa), tetramer (16kDa) and upper size band respectively. As expected, lenti-APPsw_GFP transduced cells strongly secreted 4, 8, 12kDa A β s and other A β oligomers into the culture media compared to untransduced cells (Fig. 3E)^{11,59}.

To evaluate the viability of hNSCs treated with naturally secreted A β oligomers, we cocultured hNSCs in the conditioned media of uninfected SK-N-MC cells or lenti-APP695sw_GFP infected SK-N-MC cells. When hNSCs were incubated in conditioned media from lenti-APP695sw_GFP infected cells for 72hours, their viability was significantly decreased compared to those treated with conditioned medium from uninfected cells (Fig. 4A). Next, to assess whether naturally secreted A β oligomers affect proliferation of hNSCs, cells were cultured in conditioned medium containing BrdU, which is a thymidine analogue that is incorporated into the newly synthesized DNA of cells that are in the S-phase. After coculture 72hours, hNSCs were dissociated into single cells, stained with FITC-conjugated BrdU antibodies and analyzed by flow cytometry. Human NSCs cocultured with conditioned medium from lenti-APPsw_GFP infected and uninfected cells exhibited 25.55% and 46.55% BrdU

positivity among total cells, respectively (Fig. 4B). Therefore, proliferation of hNSCs were half decreased when cells were treated with conditioned medium of lenti-APPsw_GFP infected cells. The apoptotic induction of A β oligomers on hNSCs was determined by TUNEL assay. Naturally secreted A β oligomers did not change the content of TUNEL-positive cells (Fig. 4C). Senescent cells remain viable and bioactive, but the culture in its entirety irreversibly lose its ability to divide. To analyze the senescence of hNSCs exposed to conditioned media containing naturally secreted A β oligomers, we quantified the relative degree of senescence between hNSCs cocultured with either conditioned media of lenti-APPsw_GFP transduced or nontransduced cells by measuring senescence-associated β -galactosidase activity. The A β oligomers significantly increased β -galactosidase activity at pH4.5 or 6.0. As a negative control, the sample removed the activity by heating (Fig. 4D). These results suggest that A β oligomers secreted from APP expressing cells decrease hNSC proliferation through induction of a senescence.

To test the effect of A β oligomers on the fate of hNSCs, cells were plated on PLL coated dishes without mitogen and cocultured with the conditioned media derived from uninfected SK-N-MC cells or lenti-APPsw_GFP infected SK-N-MC cells for 7days. To identify the differentiation of hNSCs, we performed immunostaining with the following antibodies: nestin for immature cells; tujl and NF for neurons; APC-CC1 for glia; GFAP, s100 β and GS for astrocytes; and O4, GalC, PDGFR- α for oligo progenitors (Fig. 5). Intriguingly, hNSCs, treated with conditioned media of lenti-APPsw_GFP transduced cells, differentiated into the glia. The hNSCs exposed to A β oligomers exhibited a decline of nestin-positive cells, whereas the number of Tuj1-positive cells did not change (Fig. 6A). To confirm the immunolabeling data, we isolated total RNA from hNSCs incubated with each conditioned medium for 7days; RT-PCR analysis was subsequently performed to show the fate of cell. The comparative changes in Tuj1, nestin, GFAP, s100 β and GS upon oligomeric A β treatment were consistent with those of immunocytochemistry (Fig. 6B). Furthermore, we monitored the upregulation of not only the level of ID1 and ID3, which are transcriptional factors involved in astrogenesis, but also that of NG2 and olig2, which are involved in oligogenesis, when hNSCs were exposed to the cultured medium of lenti-APPsw_GFP infected cells (Fig. 6B). The expression of the neuronal specific gene, *SCG10*, did not change (Fig. 6B). Therefore, naturally secreted A β oligomers enhance gliogenesis of hNSCs.

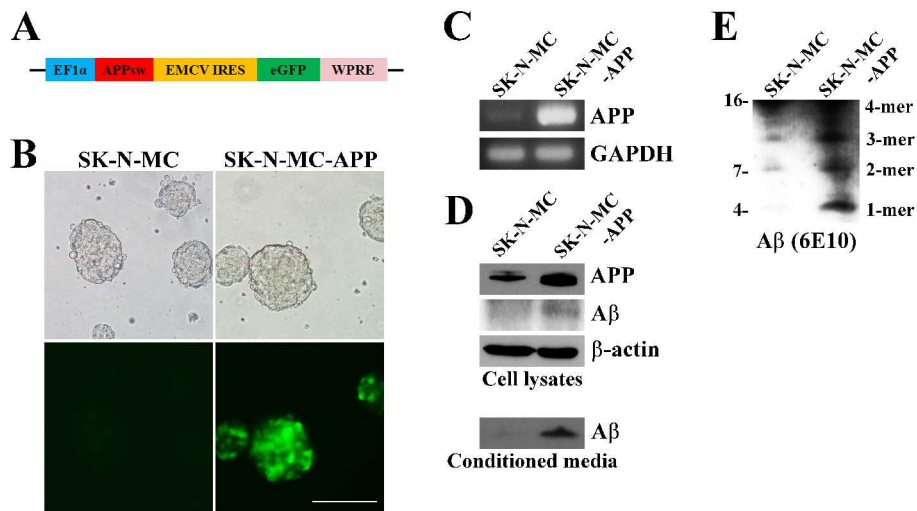


Figure 3. Generation of naturally secreted A β oligomers

(A) Schematic representation of the lenti-viral vector construct expressing human APP695 Swedish mutant (APP^{sw}). The lenti-viral vector contains EF1 α promoter and APP^{sw} followed by the EMCV-IRES, which directs translation of a eGFP.

(B) Uninfected SK-N-MC cells and lenti-APP^{sw}_GFP infected SK-N-MC cells form sphere when the cells are cultured in N2 medium without mitogen. Green fluorescent cell spheres are stably detected at 1 month after lenti-APP^{sw}_GFP infection, and uninfected SK-N-MC cells do not absolutely express the GFP. Scale bar=100 μ m.

(C) Expression of the APP gene on RT-PCR. RT-PCR is performed with the RNA from lenti-APP^{sw}_GFP infected and uninfected SK-N-MC cells. Lenti-APP^{sw}_GFP transduced cells express much greater APP than untransduced cells.

(D) APP and A β immunoblot of cellular lysates or conditioned media from SK-N-MC cells infected with lenti-APP^{sw}_GFP. Lenti-APP^{sw}_GFP infected cells significantly produce APP and A β , and predominantly secrete A β into the culture media.

(E) Identification of naturally secreted A β oligomers in conditioned medium derived from lenti-APP^{sw}_GFP infected SK-N-MC cells. Conditioned medium obtained from lenti-APP^{sw}_GFP infected cells and uninfected cells are immunoprecipitated, and immunoblotted with 6E10 (epitope: A β residues 6-10). A β oligomers are strongly exhibited in the conditioned medium of lenti-APP^{sw}_GFP infected cells compared to those of uninfected cells. SK-N-MC-APP, lenti-APP^{sw}_GFP transduced SK-N-MC cells; SK-N-MC, untransduced SK-N-MC cells

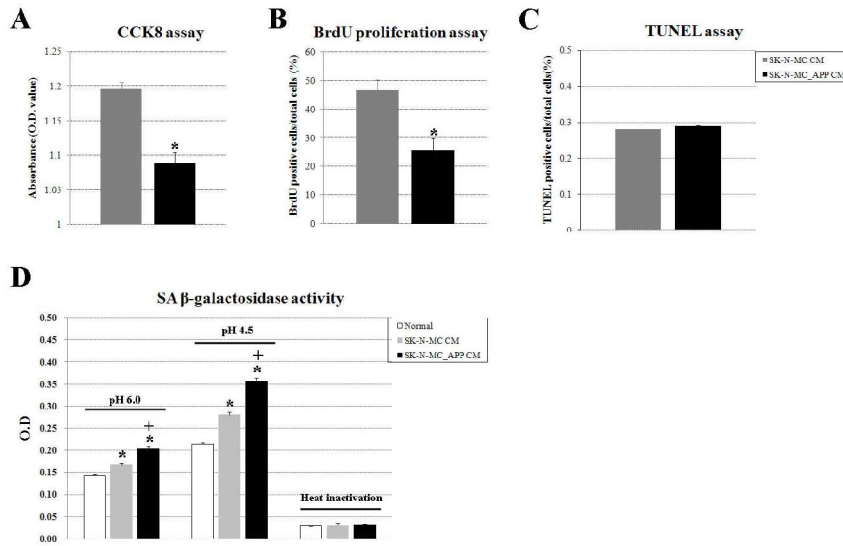


Figure 4. The proliferation of hNSCs is decreased when to expose naturally secreted A β oligomers derived from lenti-APPsw_GFP infected SK-N-MC cells.

(A) Mitochondrial function of hNSCs is decreased by the conditioned media originated from lenti-APPsw_GFP infected SK-N-MC cells. The hNSCs, treated with the conditioned medium derived from lenti-APPsw_GFP transduced cells, significantly show reduction of mitochondrial function compared to the conditioned medium of uninfected cells. Bars are the mean \pm S.E.M. * p <0.05 (Mann Whitney test).

(B) BrdU-positive hNSC are half reduced by the conditioned media from lenti-APPsw_GFP infected SK-N-MC cells comparing to untransduced cells. Bars are the mean \pm S.E.M. * p <0.05 (Mann Whitney test).

(C) Naturally secreted A β oligomers do not promote hNSC apoptosis. Cells treated with both conditioned medium rarely generate apoptosis using the TUNEL assay. Bars are the mean \pm S.E.M. * p <0.05 (Mann Whitney test).

(D) A β oligomers from lenti-APPsw_GFP infected SK-N-MC cells induce senescence of hNSCs. Bars are the mean \pm S.E.M. * p <0.05, Normal vs SK-N-MC CM or Normal vs SK-N-MC_APP CM; + p <0.05, SK-N-MC CM vs SK-N-MC_APP CM (Mann Whitney test); SK-N-MC CM, hNSCs co-cultured with conditioned medium derived from untransduced SK-N-MC cells; SK-N-MC_APP CM, hNSCs co-cultured with conditioned medium derived from lenti-APPsw_GFP transduced SK-N-MC cells; O.D., optical density.

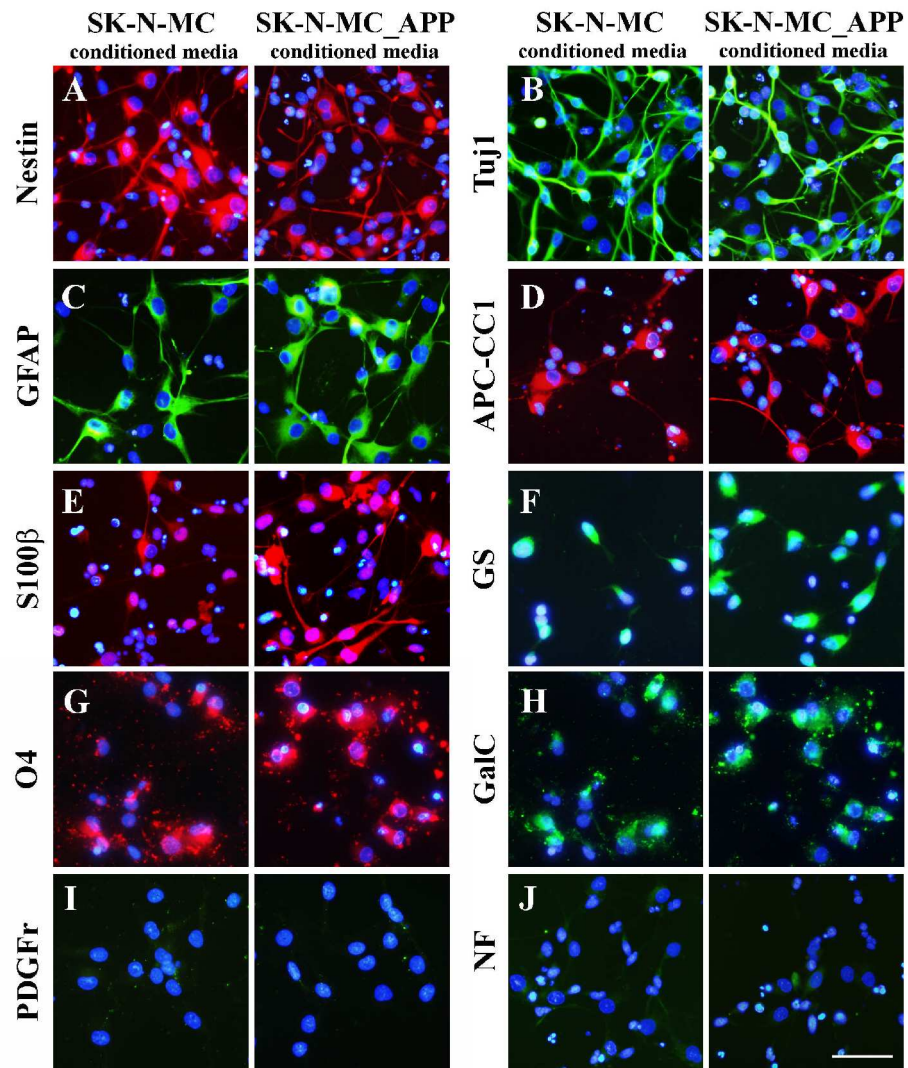


Figure 5. The conditioned media of lenti-APPsw_GFP infected SK-N-MC cells alters the fate of hNSCs. Scale bars=50 μ m.

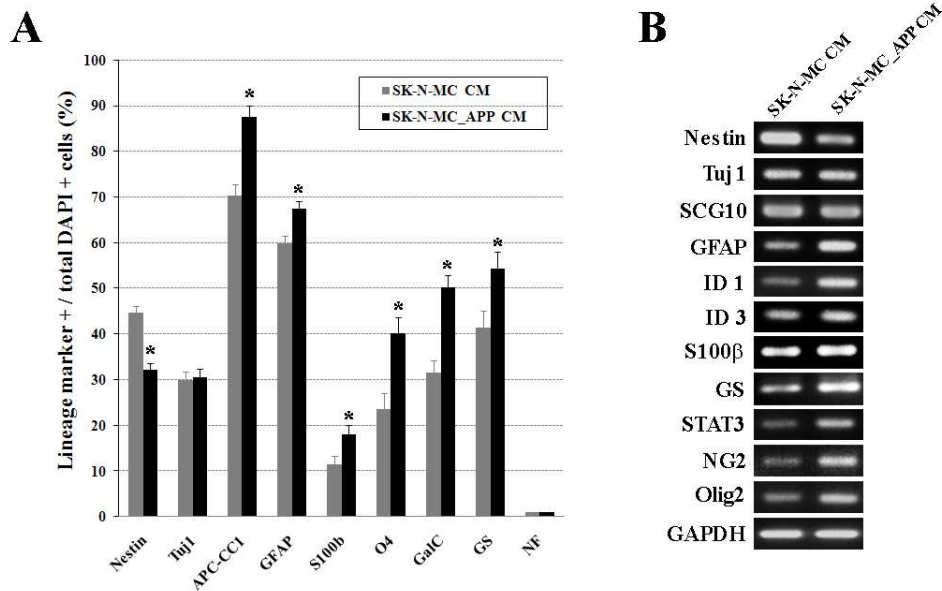


Figure 6. Naturally secreted A β oligomers induce gliogenesis of hNSCs.

(A) When hNSCs were treated with the conditioned media of lenti-APPsw_GFP infected SK-N-MC cells, the percentage of GFAP+, S100 β +, and GS+ cells are 67.49%, 18.11%, and 54.35% respectively. On the other hand, hNSCs treated with the conditioned media of uninfected SK-N-MC cells composed of 59.87% GFAP+ cells, 11.5% S100 β + cells, and 41.38% GS+ cells. Moreover, hNSCs cocultured with the conditioned media of lenti-APPsw_GFP infected cells significantly showed 40.07% O4+ and 50.2% galC+ cells compared to 23.6% O4+ and 31.58% GalC+ cells in hNSCs incubated with the conditioned medium of uninfected cells. APC-CC1+ hNSCs are statistically increased from 70.21% to 87.50% exposing to the conditioned medium of lenti-APPsw_GFP infected cells. The percentage of Tuj1+ and NF HML+ cells are similarly detected in the treatment with each conditioned medium. The significant reduction of nestin+ hNSCs by the exposure of naturally secreted A β oligomers is calculated from 44.71% to 32.22%. Bars are the mean \pm S.E.M. *p<0.05 (Mann Whitney test).

(B) Differential regulation of transcription by the conditioned medium of lenti-APPsw_GFP infected SK-N-MC cells on the RT-PCR analysis. Gene expression of nestin, Tuj1, GFAP, S100 β , and GS are correlated with immunocytochemistry. *SCG10* encoding have no change in two conditioned medium, and NG2 expressing is

elevated by incubation with the conditioned media derived from lenti-APP^{sw}_GFP infected cells. The conditioned media containing naturally secreted A β oligomers predominantly escalate the gene levels of ID1, ID3, STAT3, and olig2 related to gliogenesis. SK-N-MC CM, hNSCs cocultured with conditioned medium obtained from untransduced SK-N-MC cells; SK-N-MC_APP CM, hNSCs co-cultured with conditioned medium originated from lenti-APP^{sw}_GFP transduced SK-N-MC cells.

3. Transgenic mice carrying NSE-controlled APPsw present AD-like pathology.

The human APP mutations associated with early-onset AD enhance cleavage by the β and γ secretases, which in turn is tightly related with AD-like neuropathological changes^{7,15}. The human APP695 Swedish mutant was expressed in this APPsw tg mice under the control of the NSE promoter (Fig. 7E). According to a previous report, 12-month-old APPsw tg mice presented behavioral deficits in a water maze⁵⁵. We tested APP, A β 42, and pTaul levels in the brain of 13-month-old APPsw tg and aged matched wild mice. First, APP immunoreactivity appeared to be strong in the cortex and hippocampi of APPsw tg mice, but the same regions of wild mice showed weak immunoreactivity at the age of 13 months (Fig. 7A). Second, intracellular A β 42 immunolabeling in the cortex and hippocampus was greater in the APPsw tg mice than in wild ones; however A β plaques rarely developed in both mice (Fig. 7B). In fact, the pathogenic effect of plaques is currently being questioned, because plaque formation is not well correlated with the incidence of AD and many mouse models of AD show memory impairment long before such plaques are detected in the brain^{61,62}. In addition, it is of emerging interest that the intracellular accumulation of A β can contribute to AD progression in human brains and mouse models⁶³. The detection of A β 42 in wild mice suggests A β 42 levels are increased with age. Therefore, the APPsw tg mice reasonably reflect the AD-like pathology related to A β . Third, a phospho-tau antibody that detects the phosphorylation of tau at Thr231 was used in the immunohistochemistry of both APPsw tg and wild mice. APPsw tg mice showed an increase of phosphorylated tau compared to wild mice (Fig. 7C). In the immunoblot analyses, APPsw tg mice exhibited upregulated APP, A β , and phospho-tau (phosphorylation at Ser404 or Thr231) levels (Fig. 7D). We also observed high expression of human APP695 Swedish mutants in the brains of APPsw tg mice; however, other tissues, including the heart, liver, lungs, intestines and kidneys, did not generate human APPsw mutants upon RT-PCR analysis because the NSE promoter induces the neuron specific expression of the mutant (Fig. 7F). These data characterize APPsw tg mice as an AD animal model that is corroborated by previous studies⁵⁵.

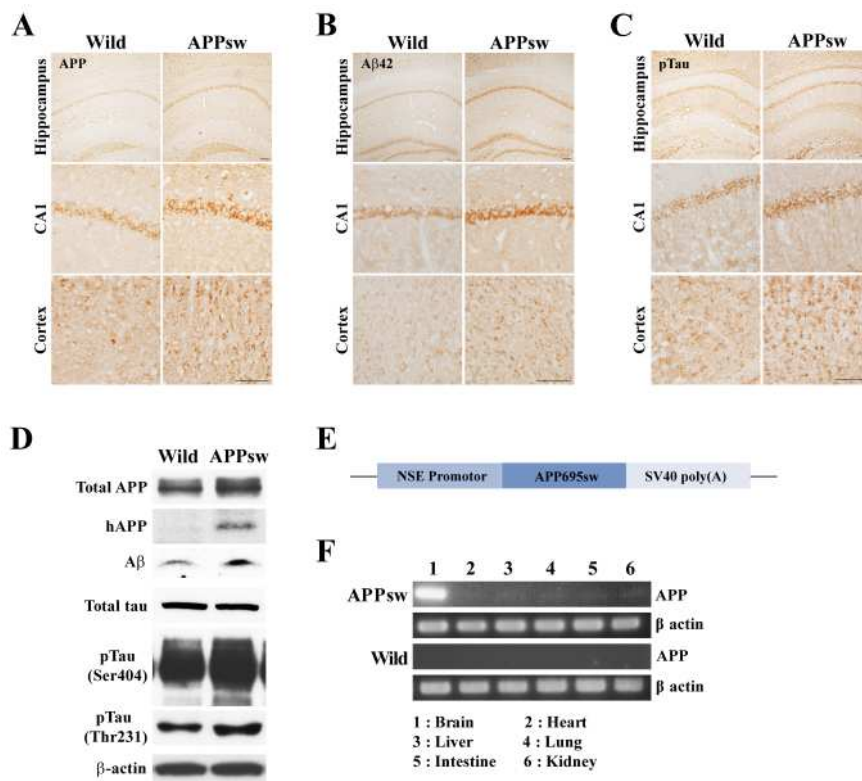


Figure 7. APPsw tg mice show AD-like pathogenic phenotype.

(A) Immunolabeling against APP in the cortexes and the hippocampi is strongly enhanced in APPsw tg mice when compared to wild mice. Scale bars=100 μ m

(B) A β 42 immunoreactivity is first detected intracellularly within the cortexes and the hippocampi. APPsw tg mice show higher density than wild mice when staining with A β 42 antibodies, but A β plaques were not observed. Scale bars=100 μ m

(C) Following staining with phosphorylated tau (AT180) antibodies, APPsw tg mice enhance immunoreactivity compared to wild mice in the cortexes and the hippocampi. Scale bars=100 μ m

(D) On immunoblot, the levels of total APP, human APP, and A β increase in APPsw tg mice. Phosphorylation of tau is relatively enhanced in APPsw tg mice compared to wild mice. Scale bars=100 μ m

(E) Construction of the pNSE-APPsw plasmid.

(F) Expression of the APPsw gene is specifically regulated in a brain. On RT-PCR, human APPsw encoding is only detected in the brains of APPsw tg mice.

4. Human NSCs engraft, migrate, and differentiate into multiple lineages in the brains of APPsw tg mice

We investigated whether hNSCs survive, migrate, and differentiate into distinct neural cell types in APPsw tg mice. To track the donor-derived cells in the host mouse brains, we prepared hNSCs using 3 different methodologies: naive and lenti-GFP transduced hNSCs, and hNSCs labeled with BrdU for 3 days *in vitro*. Thirteen-month-old APPsw tg mice received one of the three types of hNSCs in their bilateral ventricles and were sacrificed at 7-8 weeks after transplantation. Grafting hNSCs were found with anti-GFP, anti-hnuclei (hNuc), anti-human nuclear matrix (hNuMA), and anti-BrdU antibodies using immunofluorescence analysis. Human NSC widely engrafted from the transplantation site (Fig. 8A). The brains of these mice showed that a large population of grafting hNSCs remained in the SVZ of the LV and 3rd ventricles (Fig. 8B, C, G). In addition, migrating hNSCs followed white matter tracts and were distributed within the corpus callosum, fornix, thalamus, septofimbrial nuclei, cingulum, striatum, and cortex (Fig. 8D-F, H-J). Donor-derived hNSCs were scarcely found in the hippocampus. These analyses demonstrate that transplanting hNSCs into the brains of APPsw tg mice allows cells to survive and migrate from the periphery of the transplantation region to wide area in the brain.

We examined whether hNSCs retain their differentiation potential in the brains of APPsw tg mice. Immunofluorescence staining was conducted with nestin as a marker of immature NSCs; GFAP as a marker of astrocytes; Tuj1, DCX and neurofilament H, M, and L as markers of immature and mature neurons; and PDGFr α and Olig2 as markers of oligodendrocytic progenitors. In the brains of the mouse, human-specific nestin positive cells were strongly identified (Fig. 9A). Tuj1-positive cells were colocalized with hNuMA in the peripheries of the ventricles (Fig. 9B, 10B), and a few donor-derived cells expressed Olig2 in the thalamus (Fig. 9D). Migrating hNSCs following white matter tracts expressed GFAP on immunoperoxidase staining (Fig. 9C). Most of the hNSCs expressed nestin in the cortex, while others did GFAP (Fig. 10A, E). Human NSCs in white matter tracts partially expressed DCX or PDGFr α (Fig. 10C, D), and there was no neurofilament-positive hNSCs anywhere.

Therefore, hNSCs into the brains of 13 month old APPsw tg mice mainly results in undifferentiated cells, although donor-derived hNSCs partially stained with neuronal or glial antibodies (Fig. 9E)

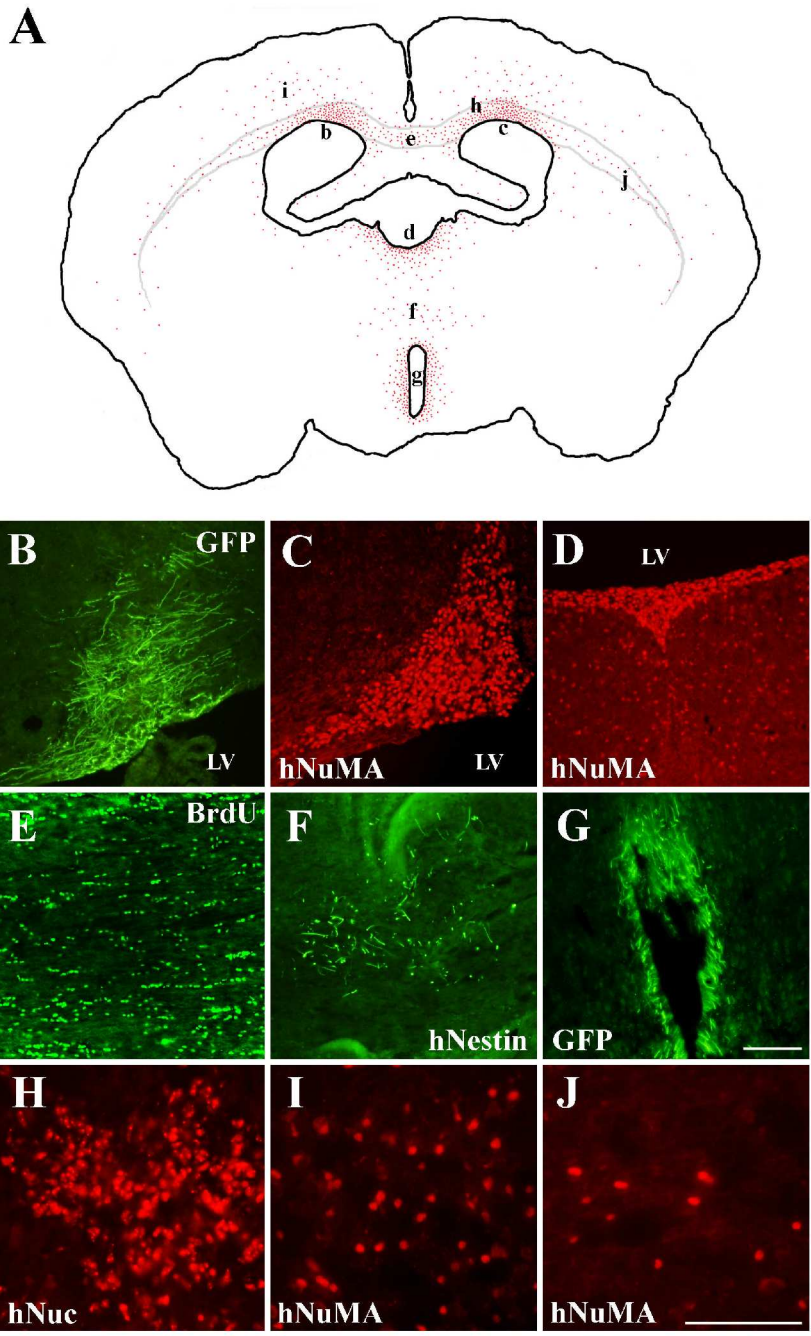


Figure 8. Engraftment of hNCSs transplanted into the LVs of APPsw tg mice

(A) Schematic graph of a representative coronal section illustrating the distribution of hNuMA positive hNSCs in the brains of APP^{sw} tg mice

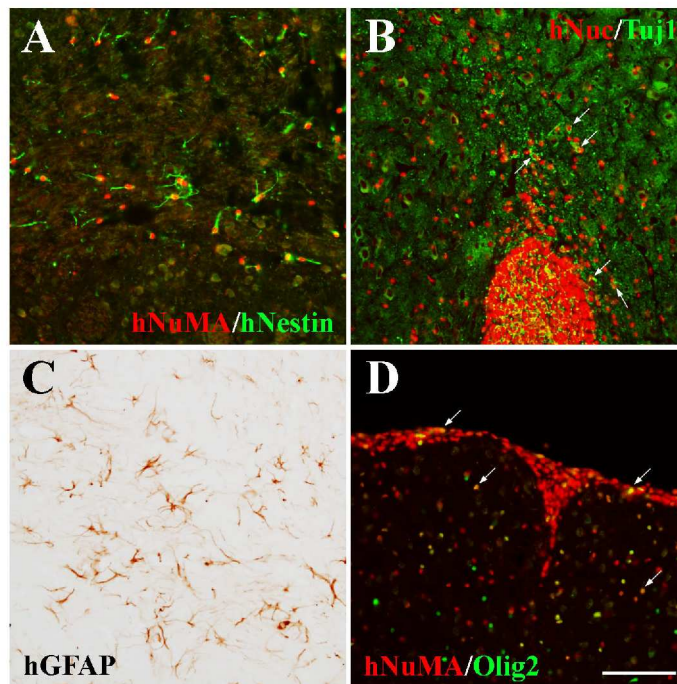
(B-C) Transplanting hNSCs are respectively found with immunoreactivity of GFP (green) and hNuMA (red) in the SVZ of the mouse.

(D) Immunofluorescence staining with hNuMA (red) reveals integration of hNSCs into the thalamus of brains of the mouse.

(E) BrdU (green) labeling hNSCs migrate from grafting sites to corpus callosum in brains of the mouse.

(F-G) On immunofluorescence staining with hNestin or GFP (green), hNSCs engraft into SVZ or periphery of 3rd ventricle.

(H-J) Immunofluorescence staining with hNuc and hNuMA (red) reveals a distribution of grafting hNSCs into the cortexes of the mouse. Scale bars=100 μ m; hNuMA, human specific nuclear matrix; hNuc, human specific nuclei.



E The fate of grafted hNuMA positive cells in the brain of APPsw tg mice

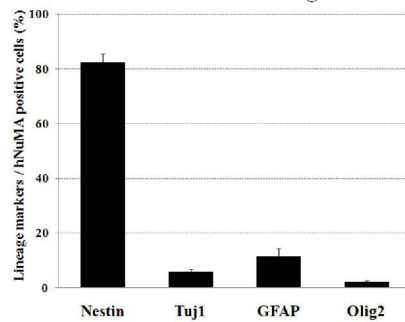


Figure 9. Donor-derived hNSCs differentiate into neurons, astrocytes, and oligodendrocytes in the brain of APPsw tg mice.

(A) Integrated hNuMA positive cells mainly show hNestin positivity.

(B) The minority of migrating hNSCs from LV are labeled with TuJ1 antibodies.

(C) Human NSCs follow white matter tracts and express GFAP.

(D) Engrafted hNuMA positive cells from LV to thalamus partially revealed Olig2 positivity. Scale bar=100 μ m

(E) Cell fate composition of hNuMA positive hNSCs in the brains of the mouse. Engrafted hNuMA positive cells respectively express neuronal marker; Tuj1 ($5.84\pm 0.88\%$), astroglial marker; GFAP ($11.67\pm 2.76\%$), oligodendroglial marker; Olig2 ($2.25\pm 0.40\%$) and undifferentiated NSC marker; nestin ($82.42\pm 3.26\%$). Bars are the mean \pm S.E.M.

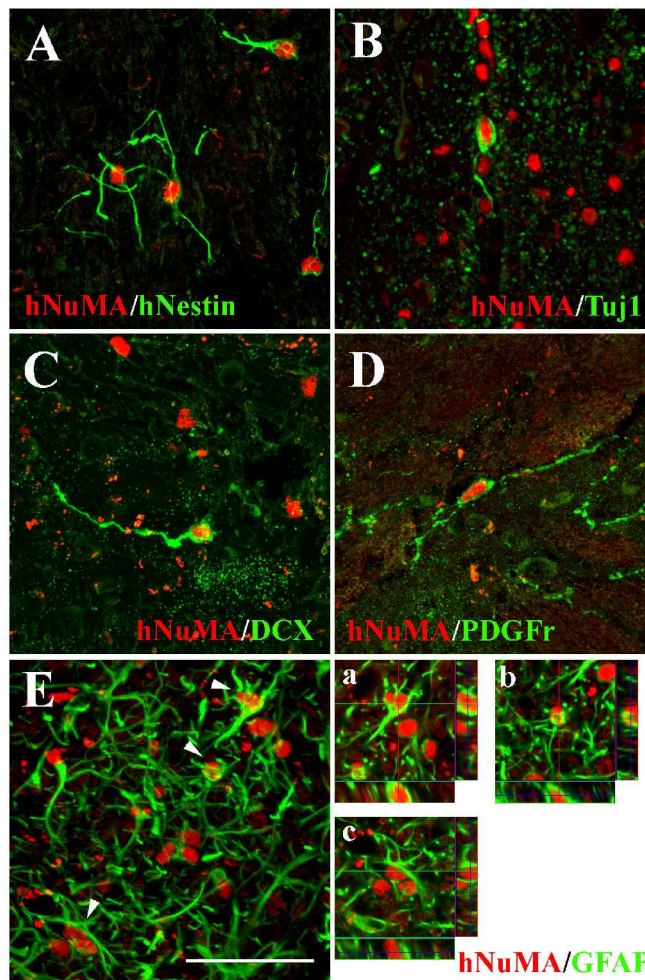


Figure 10. Differentiation of grafted hNSCs into neurons and glial cells.
 (A) Most of transplanting hNuMA positive cells remain immature cells colocalized with hNestin.
 (B) A few hNuMA positive cells concomitantly stain with Tuj1 antibodies.
 (C, D) Migrating hNuMA positive cells followed white matter track respectively co-express doublecortin (DCX) or PDGFr α .
 (E) On confocal microscopy, the minority of hNuMA positive cells have immuno-reactivity with astrocytic marker; GFAP. Arrow head shows co-labeling hNuMA and GFAP. (a-c) are images of Z-stack. Scale bar=50 μ m;

5. Transplantation of hNSCs ameliorates spatial memory, motor learning, and female forelimb strength of APPsw tg mice

We examined circadian, motorial, emotional, and cognitive change among the following 4 groups of mice at 5 weeks post transplantation. hNSC grafted APPsw tg (APP-hNSC), H-H buffer injected APPsw tg (APP-Vehicle), hNSC grafted age matched wild (Wild-hNSC), and H-H buffer injected age matched wild mice (Wild-Vehicle); all treatments were injected into the LVs of the brain.

First, we measured the ambulatory and stereotypic activities in the chamber for 22 hours. The ambulatory activity was counted as walking across the square, and the stereotypic activity was counted as swaying from one side to the other. There was no significant interaction among groups when daytime and nighttime activity, and nocturnality were compared using recorded ambulatory and stereotypic data. However, Wild-hNSC exhibited lower nighttime activity than the other groups with respect to ambulatory activity counting, and APP-Vehicle exhibited slightly higher nighttime activity than the other groups with respect to stereotypic activity counts (Fig. 11A).

Second, we examined the average latency to fall from a wire as a the measurement of forelimb strength. There were no significant differences among groups, but the weight of mice had a serious effect on latency in this test. We only analyzed female data because male weights are much more variable and heavy. Interestingly, APP-Vehicle exhibited a significant reduction of latency compared to Wild-Vehicle; APP-hNSC exhibited improved latency among female APPsw tg mice (Fig. 11B).

Third, we had the mice perform an accelerating rotarod task to evaluate motor coordination and learning through the latency to fall off of the rod. Some mice simply fell as soon as they were placed on the rod and subsequently refused the test; they were excluded as outliers in the statistical analysis. These groups showed no significant differences in latency, but APP-hNSC showed better skill acquisition than APP-Vehicle between the second and third trials (Fig. 11C).

Fourth, we carried out an open field test to evaluate spontaneous motor activity and exploratory behavior. Regarding ambulatory activity, APP-Vehicle and Wild-Vehicle exhibited significant differences in these behaviors between 20 and 25 minutes. In addition, a significant dissimilarity was found between groups in

instances of defecation, wherein APP-Vehicle defecated more than Wild-Vehicle; hNSC grafting decreased defecation, but the difference was statistically insignificant (Fig. 11D).

Fifth, we evaluated anxiety levels in an elevated plus maze consisting of 4 arms. The minority of mice occasionally entered open arms, thus, there was no relationship between the amount of time spent in open arms and the number of entries into them. There was no difference in the amount of time spent in closed arms and the number of entries into them (Table 2).

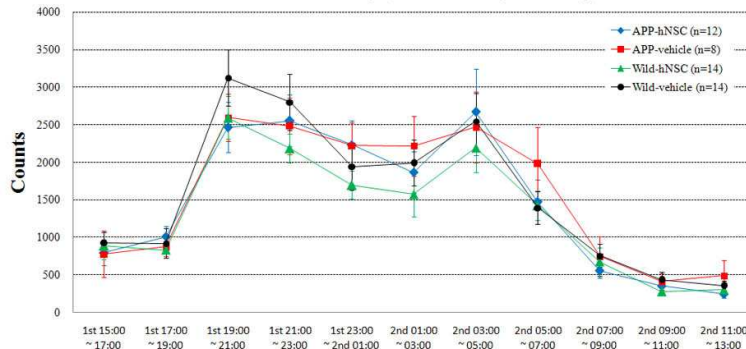
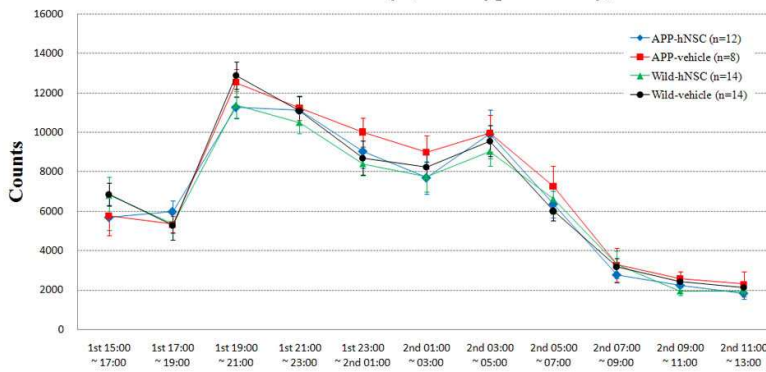
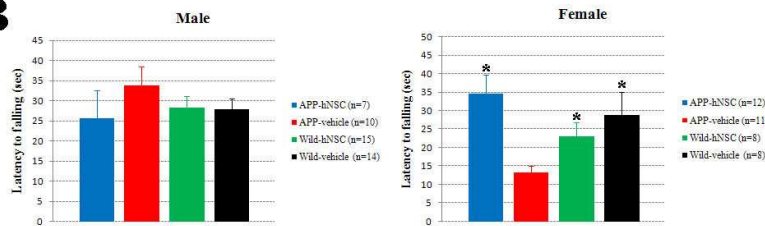
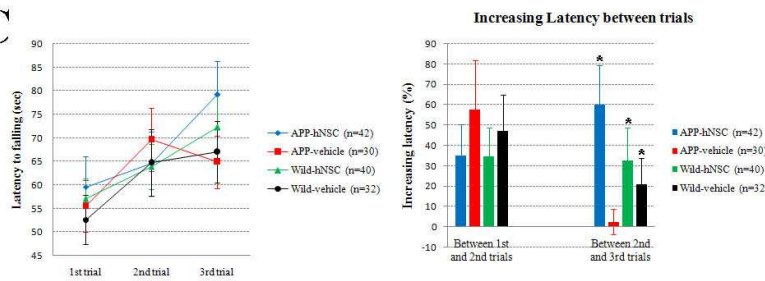
Sixth, we investigated cognitive changes in 4 groups. Acquisitional testing in the water maze with a submerged platform for 6days, revealed no differences in overall learning among the groups. On the seventh day, after 6days learning period, we measured the escape latency, which is the time spent reaching the platform region after its removal. The escape latency of APP-Vehicle was considerably longer than that of Wild-Vehicle, as expected based on a previous study. Interestingly, hNSC transplantation significantly reduced the escape latency of APPsw tg mice. All mice spent similar time in the target quadrant involved platform region (Fig. 11E). Moreover, to assess whether hNSC transplanting might interfere with the ongoing cognitive deficiency of APPsw tg mice in the long term, we performed the water maze test on 3months after hNSC or H-H buffer implantation. In the 6day learning period, APP-Vehicle recorded significantly longer acquisition times than Wild-Vehicle on the second, third, and fourth trials. In the probe test, APP-Vehicle also showed a significant decrease in spatial memory compared to Wild-Vehicle on 3months after grafting. However, APP-hNSC showed a statistical similarity to APP-Vehicle with respect to spatial memory. This suggests that the transplantation of hNSCs does not prevent the progressive cognitive impairment of APPsw tg mice until 3months after transplanting (Fig. 11F).

These results demonstrate that hNSC transplantation significantly ameliorate the impairment of forelimb strength, motor learning, and memory in APPsw tg mice. However, it does not maintain improvements in memory until 3months later.

Table 2. Effects of hNSCs transplanted into APPsw tg mice on the elevated plus maze. Bars are mean±S.E.M.

		APP-hNSC (n=19)	APP-Vehicle (n=15)	Wild-hNSC (n=18)	Wild-Vehicle (n=20)
Open arms	Entries	0.68±0.265	0.47±0.215	1.00±0.302	0.60±0.303
	Duration (sec)	18.25±8.625	8.27±4.639	13.67±4.769	12.80±9.008
Closed arms	Entries	4.58±0.880	6.07±0.892	5.67±0.554	5.6±0.727
	Duration (sec)	251.11±12.630	260.13±7.037	239.83±14.777	238.4±17.541
Open/total ratio	Entries (%)	12.49±4.376	3.73±1.716	13.07±3.756	7.73±4.404
	Duration (%)	6.07±2.875	2.76±1.546	4.56±1.590	4.27±3.003

APP-hNSC, the group of hNSC grafted APPsw tg mice; APP-Vehicle, the group of H-H buffer injected APPsw tg mice; Wild-hNSC, the group of hNSC grafted age matched wild mice; Wild-Vehicle, the group of H-H buffer injected age matched wild mice.

A**Locomotor activity (ambulatory activity)****Locomotor activity (stereotypic activity)****B****C**

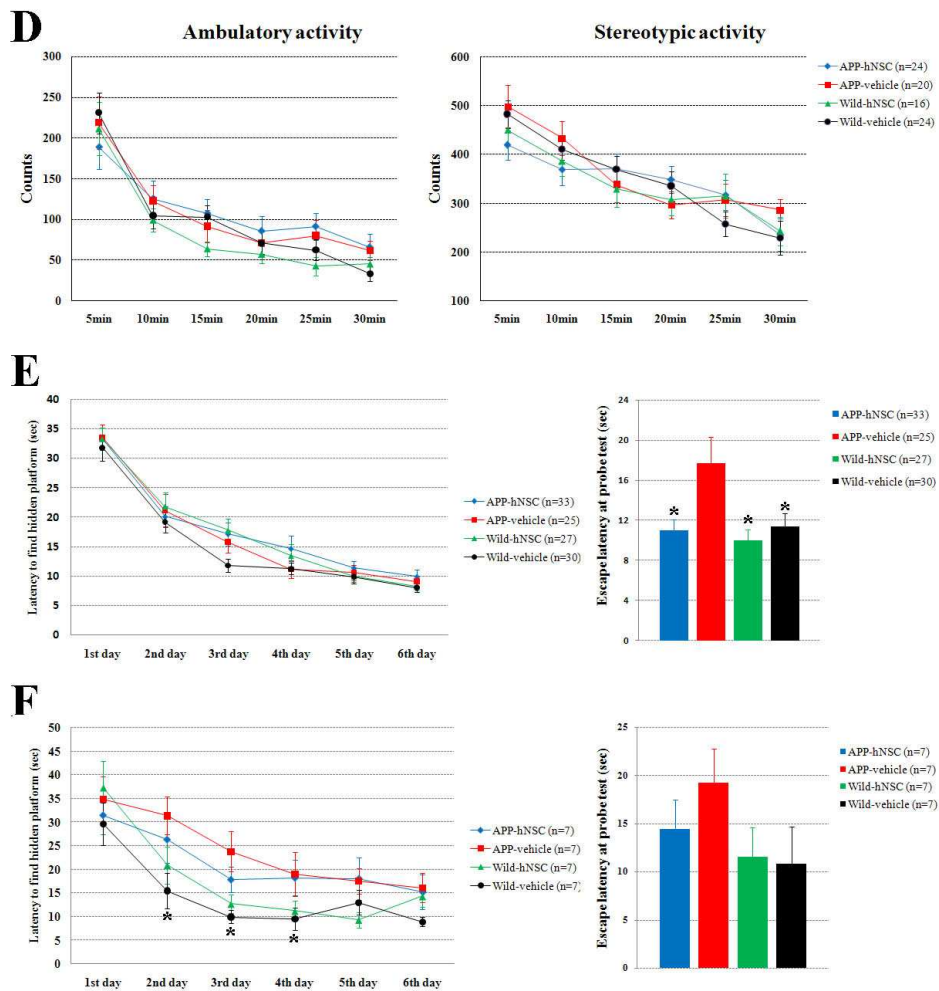


Figure 11. Behavioral phenotype of hNSC or H-H buffer transplanted mice.

(A) Locomotor activity for 22 hours. Ambulatory and stereotypic activity record movement of mice by infrared beam break detection system. Counts calculate sum of overall activity every 2 hours for 22 hours. These groups have no significant change. Bars are mean±S.E.M. (ANOVA)

(B) Wire maneuver test for 3 minutes. Because of sexual weight difference, male and female mice are separated and measured latencies before falling. In female, APP-hNSC show enhancement of forelimb strength compared to APP-vehicle. Bars

are mean±S.E.M. *p<0.05 vs APP-vehicle (Scheffe post hoc analysis on ANOVA)

(C) Elevated rota-rod test for 5 minutes. Mice of each groups perform 3 times trials. Motor skill calculate difference between trials; 1st and 2nd trial, 2nd and 3rd trial. APP-vehicle markedly impair motor skill acquisition compared to other groups. Bars are mean±S.E.M. *p<0.05 vs APP-vehicle (Scheffe post hoc analysis on ANOVA)

(D) Open field test for 30 minutes. It count ambulatory and stereotypic activity under the lighting stress. These groups have no significant change. Bars are mean±S.E.M. (ANOVA)

(E) Morris water maze at 5weeks after transplantation. For 6 day learning period, these groups show similar pattern. On the probe test, APP-hNSC significantly decrease escape latency compared to APP-vehicle. Bars are mean±S.E.M. *p<0.05 vs APP-vehicle (Scheffe post and Dunnett hoc analysis on ANOVA).

(F) Morris water maze on 3months after transplantation. In learning period, 2nd, 3rd and 4th trials significantly have difference between APP-vehicle and Wild-vehicle. On the probe test, these groups had no change, but APP-hNSC slightly decreased escape latency compared to APP-vehicle. Bars are mean±S.E.M. *p<0.05 vs APP-vehicle (Kruska Wallis and Mann-Whitney test). APP-hNSC, the group of hNSC grafted APPsw tg mice; APP-Vehicle, the group of H-H buffer injected APPsw tg mice; Wild-hNSC, the group of hNSC grafted age matched wild mice; Wild-Vehicle, the group of H-H buffer injected age matched wild mice; n, the number of individuals.

6. Transplantation of hNSCs into APPsw tg mice leads to a reduction of A β 42

To determine whether hNSCs grafted into the bilateral ventricles of APPsw tg mice affect A β 42 levels in the cortex and hippocampus, mice were euthanized at 7-8 weeks after transplantation. As a control, H-H buffer was injected using the same method described above. Although APPsw tg mice used in this study rarely present A β plaques at older ages, intracellular A β in neurons was widespread in their brains (Fig 7B). There is now abundant evidence suggesting that intraneuronal A β can disrupt synaptic activity, lead to proteasome dysfunction, cause calcium dyshomeostasis, and even facilitate the hyperphosphorylation of tau. A β 42 is much more prone to oligomerization and fibrillization in the AD brain and is much more toxic than its more abundant counterpart, A β 40. Therefore, we studied intracellular A β 42 levels by using immunoperoxidase staining. The coronal brain sections were probed with A β 42, and bound antibodies were detected by DAB reaction. Interestingly, we observed a reduction of intracellular A β 42 deposition in the cortex and hippocampi of hNSC grafted mice compared to their H-H buffer injected counterparts; however, amyloid plaques did not change between groups (Fig 12). The transplantation of hNSCs into APPsw tg mice induced A β 42 clearance not only near the cortex to retain human-specific marker positive cells (Fig 12A,B) but also in the cortex and hippocampus far from transplant sites (Fig 12C-H). The decline of A β 42 in the hippocampus was mainly presented in the CA1, and dentate gyrus. Thus, hNSCs grafting appears to play a significant role in modulating intracellular A β 42.

To quantify A β levels between hNSCs and H-H buffer implantation into the brains of APPsw tg mice, we prepared T-PER soluble (detergent soluble) and 70% formic acid (detergent insoluble) extracts from the 2 experimental groups. In agreement with the immunohistochemistry results, ELISA analyses demonstrate that detergent soluble A β 42 peptides were significantly reduced in the brains of hNSCs grafted APPsw tg mice compared to their H-H buffer injected counterparts, although the change of detergent insoluble A β 42 peptide was not significant (Fig 13A). The level of A β 40 did not change between groups (Fig 13A). These results suggest that the transplantation of hNSCs into APPsw tg mice has a profound impact on A β 42 clearance.

To determine what factors of hNSCs cause the decrease of detergent soluble A β 42, we examined the expression of A β -degrading proteases from hNSCs both in vitro and

in vivo. We isolated total RNA from proliferating and differentiated hNSCs. Many studies has currently suggested that neprilysin (NEP), insulin-degrading enzyme (IDE), angiotensin converting enzyme (ACE), endothelin converting enzyme (ECE)1, 2 and plasminogen activators (tissue type plasminogen activator (PLAT), urokinase type plasminogen activator (PLAU)) play roles in regulating A β deposition in the brain⁶⁴. Matrix metalloproteinases (MMP) 2, 3, and 9 are also related to A β -degrading activity⁶⁵, and the cysteine protease, cathepsin B (CTSB), reduces levels of A β 1-42⁶⁶. Therefore, we performed RT-PCR with the total RNA of hNSCs obtained in vitro to confirm the encoding of these A β degradable proteins. Human NSCs on proliferation or differentiation condition produced high levels of IDE, MMP2, CTSB, PLAT, and PLAU. ECE1, ECE2, and ACE1 were differently expressed between proliferation and differentiation condition. On the other hand, NEP was slightly expressed, and the expression of MMP3, and MMP9 was not detected (Fig 13B). To evaluate the encoding of human A β degradases in the brains of hNSCs grafted APPsw tg mice, we carried out RT-PCR from APPsw tg mice brains 7weeks after hNSCs grafting. As negative controls, H-H buffer implanted APPsw tg mice were investigated in parallel. We identified the higher expression of CTSB; in addition, IDE, MMP2, ECE1, tPA, and uPA were identified with primers detecting human-specific encoding (Fig 13C). These data show that both in vitro and in vivo, the production of A β degrading proteases from hNSCs regulates A β generation and accumulation, although only small quantities of these proteins exist.

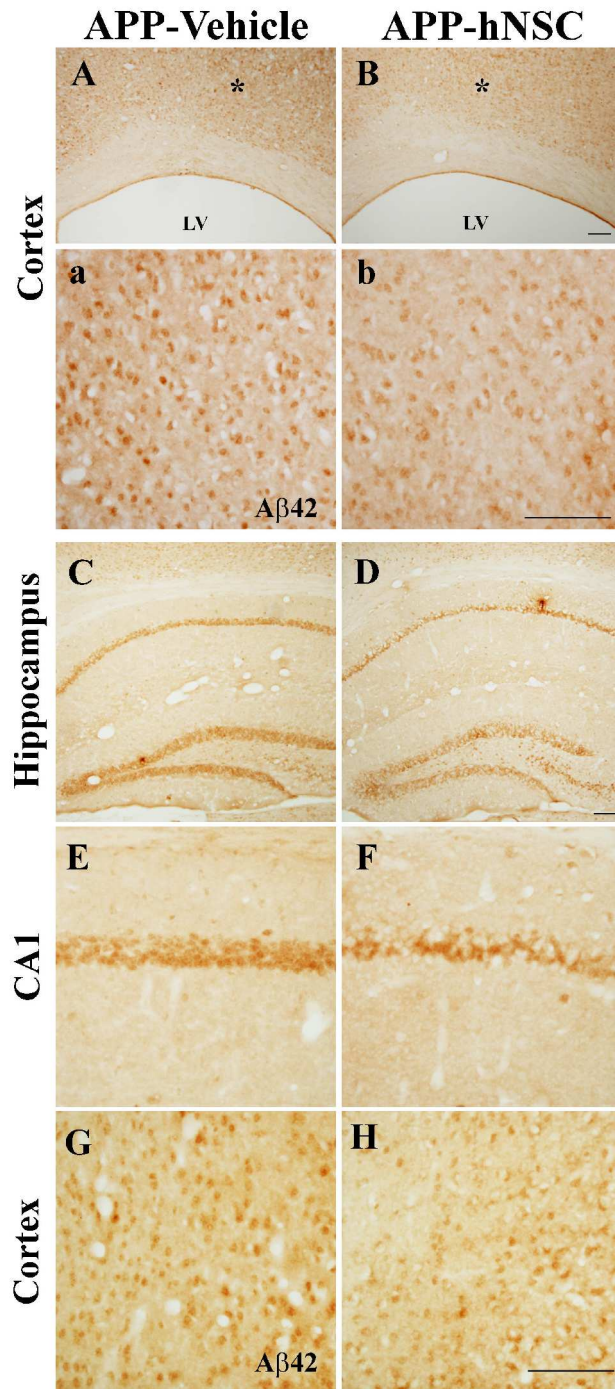


Figure 12. Intracerebroventricular injection of hNSCs reduces intracellular A β 42 aggregates in the hippocampi and cortexes of APPsw tg mice.

(A, B) Low- and high-magnification view of cortexes near the hNSC transplantation site reveal that hNSC grafting is sufficient to markedly reduce intracellular A β 42 immunoreactivity. (a, b) The region of asterisk (A,B) is magnified.

(C, D) Low-magnification view of the hippocampi show the reduction of A β 42 immunoreactivity in hNSC grafted APPsw tg mice compared to H-H buffer injected ones.

(E-H) Intracellular A β 42 levels are strongly decreased in the CA1 and cortex of hNSC grafted APPsw tg mice compared to H-H buffer injected ones. Scale bars=100 μ m; APP-vehicle, H-H buffer injected APPsw tg mice; APP-hNSC, hNSC grafted APPsw tg mice.

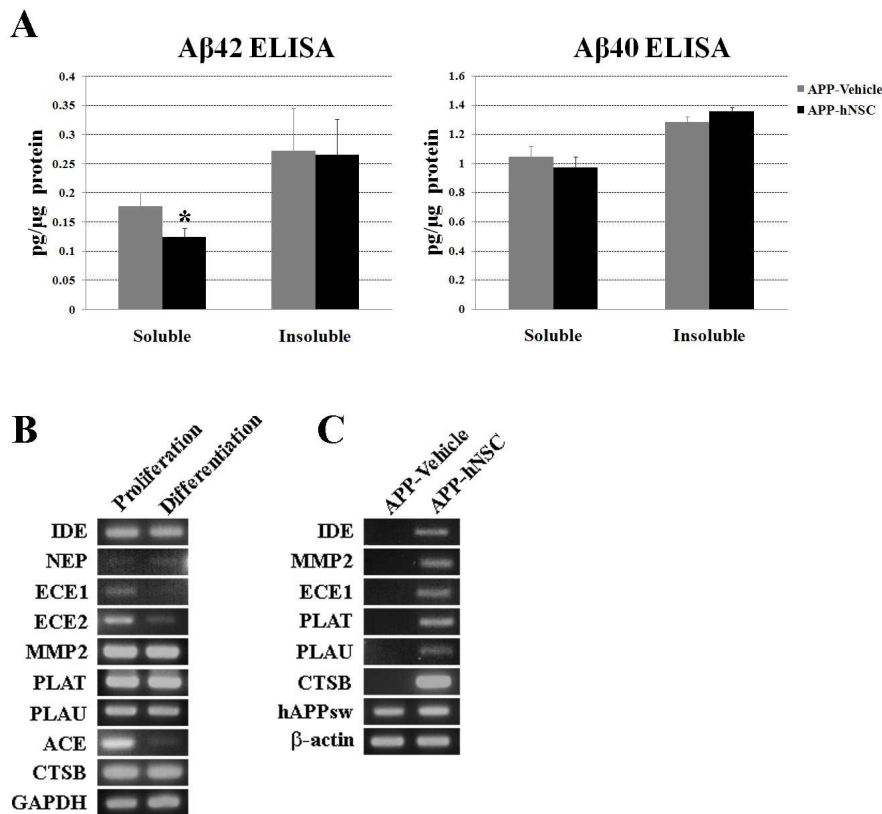


Figure 13. The transplantation of hNSCs modulates levels of A β 42 in the brains of APPsw tg mice and hNSCs express A β degradases in vitro and in vivo.

(A) Soluble and insoluble A β 40/42 are quantified by ELISA. Levels of A β 42 are significantly reduced in detergent soluble brain extracts of hNSC grafted APPsw tg mice compared to H-H buffer injected ones, but levels of insoluble A β 42 have no change between groups. ELISA for soluble and insoluble levels of A β 40 reveal no difference from brain extracts of hNSC and H-H buffer injected mice. Bars are mean \pm S.E.M. * p <0.05 (unpaired t-test)

(B) In vitro, hNSCs under proliferation or differentiation conditions generate several A β degradases; IDE, NEP, ECE1/2, MMP2, PLAT, PLAU, ACE, and CTSB on RT-PCR analysis.

(C) Human NSC transplanted into the brains of APPsw tg mouse still produce IDE, MMP2, ECE1, PLAT, PLAU, and CTSB on RT-PCR analysis. APP-vehicle, H-H buffer injected APPsw tg mice; APP-hNSC, hNSC grafted APPsw tg mice.

7. Human NSC grafting suppresses the phosphorylation of endogenous tau in APPsw tg mice

To assess the effect of hNSC administration into APPsw tg mice on tau-related pathology, we compared the phosphorylation of tau between hNSC transplantation and H-H buffer injection. We measured immunoreactivity with phosphorylated tau-specific antibodies (AT180, phosphorylated Thr231 residue; PHF13, phosphorylated Ser396 residue) on coronal brain sections and from brains extracts. Immunohistochemistry revealed a marked decrease in AT180 labeling on CA1 pyramidal neurons and the cortexes of hNSC implanted APPsw tg mice compared to H-H buffer injected counterparts (Fig. 14A-F). As expected, phosphorylated tau was also reduced as a result of hNSC grafting into the brains of APPsw tg mice upon western blot analysis, although total tau proteins were unchanged following the transplantation of hNSCs or H-H buffer (Fig. 14G). These findings indicate that phosphorylated tau aggregation is dependently modulated by hNSC grafting. Next, we analyzed the levels of phosphorylated GSK-3 β in the administration of hNSCs or H-H buffer, because GSK-3 β is a major kinase that phosphorylates tau in AD and its phosphorylation indicates an inactivated state^{67,68}. We showed that hNSC grafting induced the phosphorylation of GSK-3 β in the brains of APPsw tg mice though GSK-3 β proteins were equally expressed in both groups (Fig. 14H). Human NSCs expressed neurotrophins including BDNF, NT3, NT4/5, and NGF in vitro (Fig. 14I). These factors can interact with TrkA/B/C receptors and activate the PI-3K/Akt signaling pathway⁶⁹. Activated Akt consecutively induces the phosphorylation of GSK-3 β . Intriguingly, hNSC grafting result in higher phosphorylated levels of TrkA/B, and successively phosphorylates Akt via signal transduction cascades (Fig. 14H). These data show that neurotrophins secreted from hNSCs in the brains of the mouse induce GSK-3 β phosphorylation and inhibit GSK-3 β activity via neurotrophin/Trk signal transduction. Therefore, change of GSK-3 activity through hNSC grafting regulates tau phosphorylation in the brain of the mouse.

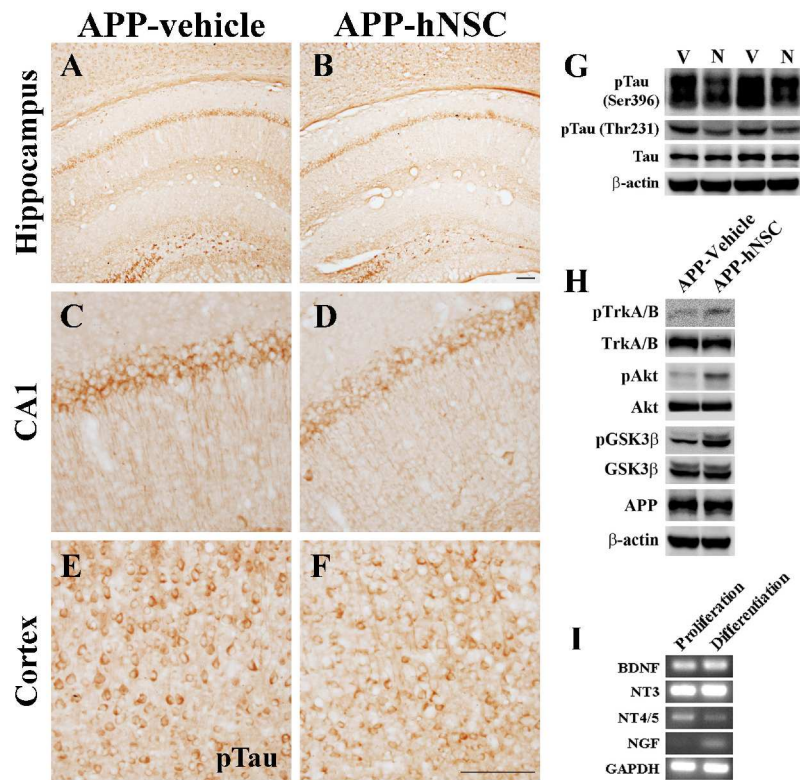


Figure 14. Reduction of phosphorylated tau and tau-related signal pathway in hNSC grafted APPsw tg mice.

(A, B) In low magnification view of the hippocampi, hNSC administration effectively reduce levels of phosphorylated tau in the mouse. Scale bars=100 μ m

(C-F) In immunoperoxidase staining, intracerebroventricular hNSC grafting significantly decrease phosphorylated tau in CA1 and cortexes of the mouse. Scale bars=100 μ m

(G) Brain extracts from hNSC transplanted the mice reduce band intensity of phosphorylated tau (phophorylated Thr231, Ser396 residue) in the western blot analysis.

(H) According to PI-3K/Akt signaling pathway, phosphorylation of TrkA/B, Akt and GSK3 β are strongly observed in hNSC grafted the mice compared to H-H buffer injected ones in the western blot analysis.

(I) In vitro hNSCs under proliferation and differentiation conditions expressed neurotrophins; BDNF, NGF, NT3, NT4/5 in RT-PCR analysis. APP-vehicle, V, H-H buffer injected APPsw tg mice; APP- hNSC, N, hNSC grafted APPsw tg mice.

8. Transplantation of hNSCs in APPsw tg mice attenuates astrogliosis and microgliosis.

To examine whether hNSC grafting alters astrogliosis and microgliosis in APPsw tg mice, we performed immunostaining of astrocytes and microglia because A β deposits and oligomers promote the activation of astrocytes and microglia in AD^{11,21,70}. To monitor brain inflammation, we used GFAP as a marker of astrocytes, and studied microglial activation with CD11b, F4/80, and Iba-1 antibodies, especially in the motor cortex, which was efficiently engrafted by the hNSCs, and hippocampus. A reduction of astrogliosis was significantly detected in the hippocampi of hNSC graft compared to H-H buffer injection when measuring the intensity of GFAP labeling to quantify astrogliosis (Fig. 15A-C). We also found that the immuno-reactivity against CD11b and F4/80 was lessened in the hippocampi of hNSC grafted the mice (Fig. 16A-D). Other microglial marker, Iba1, provided similar results to those of CD11b and F4/80 in the hippocampus (Fig. 16G-J). In addition, Iba1-positive cells, which presented more active morphology, were decreased in the motor cortexes of hNSC grafted the mice compared to H-H buffer injected ones (Fig. 16E, F). The number of microglial cells between hNSC and H-H buffer administration was significantly different; in particular, Iba1-positive cells were decreased by hNSCs grafting (Fig. 16K). Therefore, these data demonstrate that hNSC administration decreases inflammation in the brains of APPsw tg mice and does not provoke immune rejection. Next, we performed in vitro studies to check the expression of anti-inflammatory cytokines secreted from hNSCs⁷¹. Human NSCs were incubated with pro-inflammatory cytokines including TNF α , IFN γ , and IL1 β ⁴⁶. After 24 and 48 hours, cells were collected and prepared for RT-PCR analysis. We found that hNSCs generated a wide range of anti-inflammatory cytokines (Fig. 16L). IL10 was slightly expressed during proliferation conditions at 48hours, and IL1 receptor antagonist was strongly expressed during proliferation and differentiation when treated with pro-inflammatory cytokines. IL4 was gradually upregulated during differentiation from 24 to 48 hours, whereas it was slowly downregulated during proliferation. Interestingly, TGF β was always highly expressed regardless of exposure of pro-inflammatory cytokines. These data suggest that hNSCs in the inflammatory environment secrete anti-inflammatory cytokines and can modulate neuroinflammation.

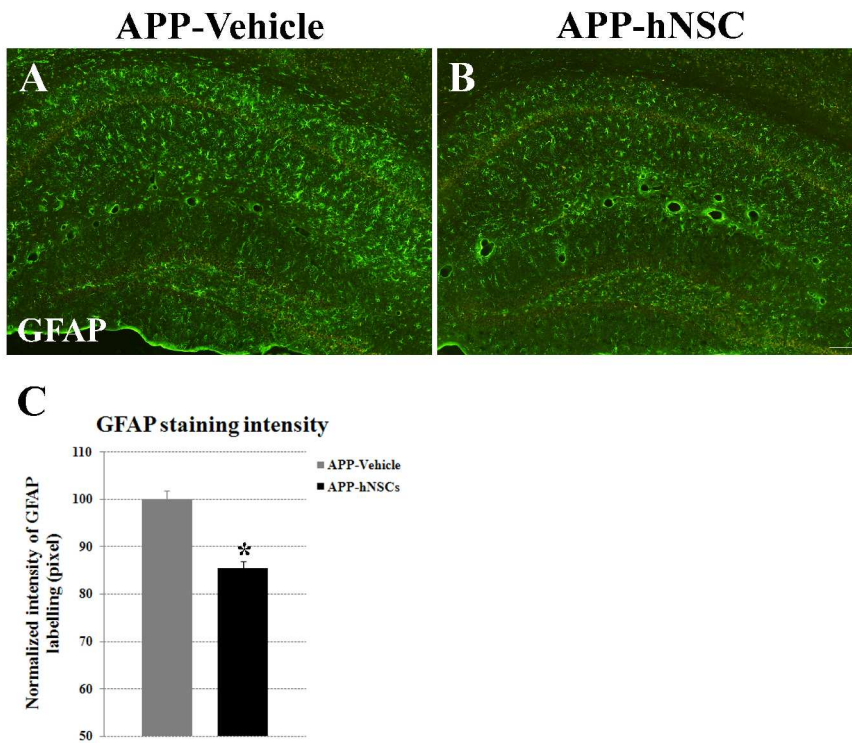


Figure 15. Analysis of astrogliosis in the brain of hNSC grafted and H-H buffer injected APPsw tg mice

(A, B) GFAP immunoreactivity in hippocampi of hNSC grafted the mice is reduced when compared to H-H buffer injected ones. Scale bars=100 μ m

(B) Quantitative analysis of GFAP staining intensity. Transplantation of hNSCs significantly inhibits astrogliosis. When a GFAP labelling level of hNSC grafted group are normalized by the level of H-H buffer injected group, hNSC grafting induce 15% decrease in the hippocampus. Bars are sem \pm S.E.M. *p<0.05 (unpaired t-test). APP-vehicle, H-H buffer injected APPsw tg mice; APP-hNSC, hNSC grafted APPsw tg mice.

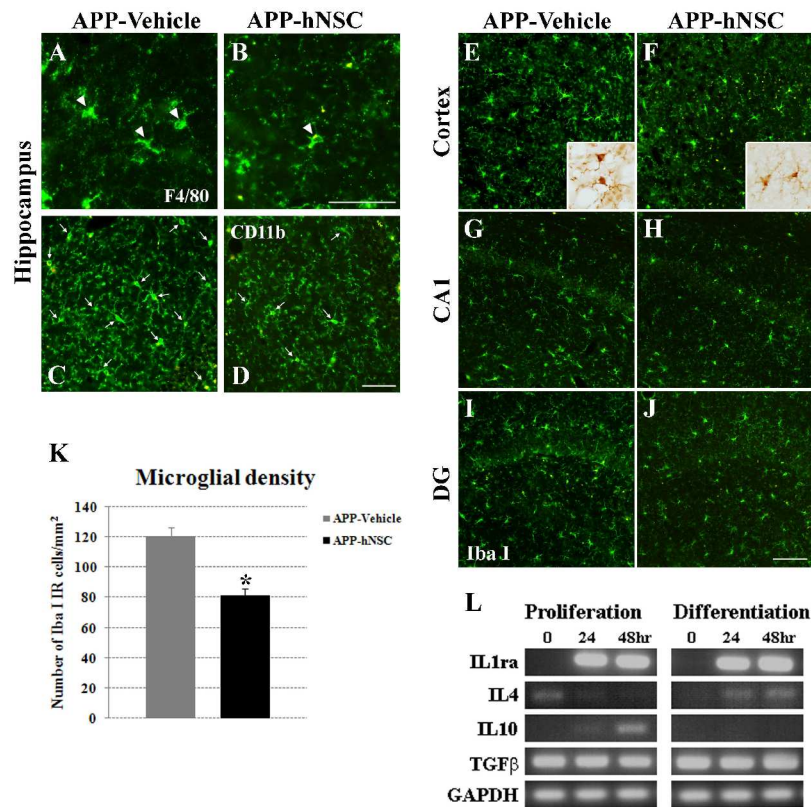


Figure 16. Analysis of microglial activation in hNSC grafted and H-H buffer injected APPsw tg mice.

(A-D) In the hippocampus, hNSC graft decreases the number of F4/80 and CD11b positive cells in the comparison of H-H buffer injection. Arrow and arrow head direct active microglia. Scale bars=50 μ m

(E-J) The number of Iba1 positive cells was reduced in DG, CA1 and cortexes through hNSC graft. (insert of E and F) Microglia in hNSC grafted mice show inactive form; ramified process and small cell body. Scale bars=100 μ m

(K) Quantification of Iba1 positive cells shows a significant decrease by hNSCs administration. Bars are mean \pm S.E.M. *p<0.05 (unpaired t-test). APP-vehicle, H-H buffer injected APPsw tg mice; APP-hNSC, hNSC grafted APPsw tg mice.

(L) Exposing to IL1 β , TNF α and IFN γ for 24 and 48 hours, hNSCs express anti-inflammatory cytokines under in vitro proliferation and differentiation conditions. RT-PCR analysis showed mRNA levels of IL1ra, IL4, IL10 and TGF β .

9. Human NSCs in the brains of APPsw tg mice increase hippocampal synaptic density and host cells survival

The synapse is widely assumed to be the cellular basis for memory. Previously, soluble A β oligomers can induce the alteration of the synaptic shape, composition, and density in AD. Taking these facts, we analyzed immunoreactivity toward synaptophysin, which labels the presynaptic terminals of functional synapses, using confocal microscopy followed by optical densitometry^{11,48,62}. Human NSC grafting result in a significant 18% increase in synaptic density in the CA1 striatum radiatum of APPsw tg mice compared to H-H buffer injection (Fig 17A-C). Western blot analysis revealed that the change of synaptophysin levels was similar to what observed in immunohistochemistry (Fig 17D). Therefore, these results suggest that hNSC grafting attenuates synaptotoxic properties, thus providing cognitive improvement in APPsw tg mice.

Apoptosis has been an attractive mechanism for neuronal death in AD for several years^{14,72}. To investigate whether hNSC grafting prevent apoptosis observed in the brains of APPsw tg mice, we performed a TUNEL analysis to label apoptotic cells. A significant decrease of TUNEL-positive cells was found in hNSC grafted compared to H-H buffer injected APPsw tg mice (Fig. 18A-C). Next, we assessed the cleavage of caspase 3 as apoptotic cell marker between hNSC and H-H buffer administration to show the apoptosis in both groups. Western blot analysis revealed that hNSC grafting induced a striking decrease of active caspase 3 in APPsw tg mice (Fig. 18D). These data suggest that hNSCs can protect host cells against the degenerative environment in the brains of mice.

Neurotrophic and growth factors are considered relevant in the pathogenesis of neurological disorders that may be characterized by enhanced vulnerability and/or reduced cellular plasticity^{47,52}. In vitro, we estimated the mRNA levels of these factors during proliferation and differentiation of hNSCs. FGF2, NT3, and VEGF were predominantly secreted by cells, and the expression of NGF and GDNF were barely detected during differentiation; NT4/5 also showed mild expression (Fig. 18F). To determine whether these factors secreted by hNSCs cause changes in the host brain, we analyzed the activation of extracellular signal related kinase (Erk), which augments cell signaling related to cell survival and the functional state of neurons⁷³, in the mouse brain. Western blot analysis revealed that hNSC grafted APPsw tg mice

exhibited more phosphorylation of Erk1/2 than ones administered with H-H buffer (Fig. 18E). These data suggest that trophic and growth factors generated by hNSCs can have protective effects in the vulnerable brains of APPsw tg mice according to the signaling pathway of tyrosine kinase receptor because hNSC grafted mice exhibit higher phosphorylated TrkA/B (a tyrosine kinase receptor) compared to H-H buffer injected mice.

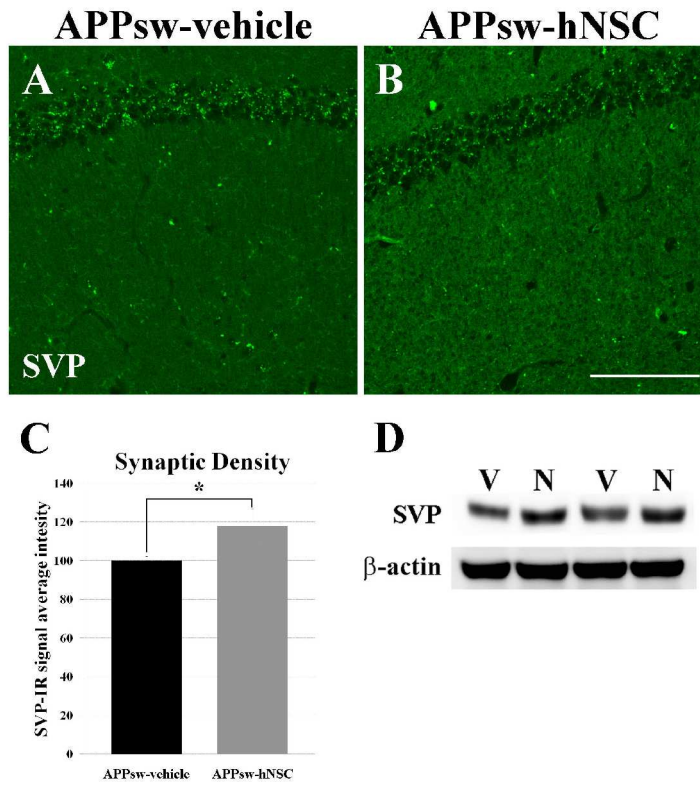


Figure 17. hNSCs augment synaptic density.

Confocal optical densitometry reveals that compared to H-H buffer injected APPsw tg mice (A), hNSC grafted APPsw tg mice (B) exhibit a 18% increase (C) in synaptophysin immunoreactivity within the striatum radiatum of CA1 (green puncta, quantified in $*p < 0.05$ (unpaired t-test)).

(D) Western blot analysis demonstrates a significant elevation of synaptophysin in hNSC grafted mice versus H-H buffer injected mice. Data in (C) is normalized to the level of H-H buffer injected APPsw tg mice and shown as $\text{mean} \pm \text{S.E.M.}$ Scale bar = $50 \mu\text{m}$. APPsw-vehicle, H-H buffer injected APPsw tg mice; APPsw-hNSC, hNSC grafted APPsw tg mice; SVP, synaptophysin; IR, immunoreactivity; V, APPsw-vehicle; N, APPsw-hNSC.

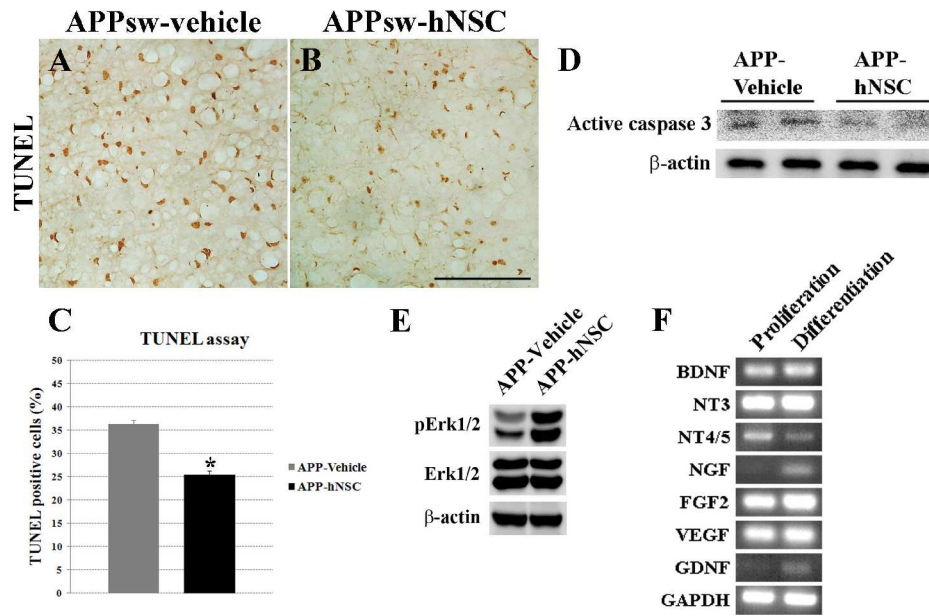


Figure 18. Human NSCs have an anti-apoptotic effect via secretion of trophic factors in the brains of APPsw tg mice.

(A,B) Image of TUNEL positive cells in the cortexes of H-H buffer and hNSCs injected APPsw tg mice. Scale bar=100 μ m.

(C) Quantification of TUNEL positive cells between hNSC and H-H buffer injecting. Data is presented as a percentage of TUNEL positive cells per total nuclei and shown as mean \pm S.E.M. *p<0.05 (unpaired t-test).

(D,E) In western blot, hNSCs down-regulate the levels of active caspase3 and induced the phosphorylation of Erk compared to H-H buffer injection in the mouse brain . APP-vehicle, H-H buffer injected APPsw tg mice; APP-hNSC, hNSC grafted APPsw tg mice.

IV. DISCUSSION

More than 35 million people worldwide have AD, which is a progressive neurological disorder^{1,13}. It is thought that two main risk factors develop AD. First, elevated A β oligomer levels or A β 42/A β 40 ratio occur synaptic dysfunction, generate neuroinflammation, disturb neuronal ionic homeostasis and progress neuronal injury⁹⁻¹¹. Second, the hyper-phosphorylated tau reduces affinity to microtubules, and consequently disrupts axonal transport¹²⁻¹⁴. Unfortunately, although several diverse approaches aimed at inhibiting the progression of AD have been proposed; including A β -related treatment, tau pathology approaches, anti-inflammatory approaches, APOE-related treatment, and metabolic dysfunction approaches^{21,24,25}, no AD therapy possesses outstanding performance at present. To overcome this limitation, one of the possible treatments is NSC based cell therapy. When NSCs are implanted into a diseased or injured nervous system, they not only exhibit extensive preferential migration to and engraftment within areas of lesions, but also the capability to replace diseased tissue in an appropriate manner^{41-45,50-52}. Apart from replacing lost cells, the administration of NSCs based therapy can provide a regenerative environment for other cells residing in the diseased brains^{44-48,52}. From this perspective, NSC grafts can potentially improve the deficits of AD. In the present study, hNSCs were isolated from human fetal telencephalon at 13 weeks of gestation; the procedure was approved by the ethics committee of Yonsei University College of Medicine⁵³. The hNSCs exist with some restricted neuronal or glial progenitors in self-renewing neurospheres as neural progenitors and radial glial cells. Furthermore, the multipotency of the hNSCs is confirmed under the condition of differentiation in vitro and through transplantation into the ALS mouse model^{53,74}. To understand the relationship between hNSCs and A β , we established SK-N-MC cells producing naturally secreted A β oligomers which are similar to the AD causable A β form in AD patients^{59,60}. Many researchers have utilized synthetic A β peptide for several years, but these peptides are different from the pathophysiological form of the AD environment^{10,61}. To remove the effect of other factors secreted from the SK-N-MC cells, we also used conditioned media from the

SK-N-MC cells as a control. The proliferation of hNSCs significantly decreased when the cells were cultured with conditioned media including A β oligomers derived from lenti-APPsw_GFP transducing SK-N-MC cells. The dramatic reduction in proliferative capacity results from senescence and not apoptosis. Although it is reported that A β oligomers are cytotoxic⁹⁻¹¹, hNSCs expressed neurotrophic and growth factors; therefore, these factors prevent hNSCs from dying via a self-stimulating trophic effect^{41,47,48,52,73,74}. Interestingly, conditioned media including naturally secreted A β oligomers induced the gliogenesis of hNSCs as observed through mRNA and protein levels. Up to date, it is unclear whether A β induce neurogenesis of NSCs and neural progenitors because experimental conditions were very different from each other⁷⁵⁻⁸¹. Furthermore, most studies investigated not only diverse concentrations and different states of A β but also utilized NSCs obtained from different species and distinct spatial-temporal points. Consequently, the effect of A β on the fate of NSCs remains controversial. A β exists in multiple assembly states that have different physiological or pathophysiological effects^{9,10,61}. Nevertheless, our results confirm that hNSCs isolated from 13week-old fetal brain differentiated into glia when treated with A β oligomers which has a striking similarity to the risky form found in AD. At present, there are no mouse models that recapitulate all aspects of AD pathogenesis. Nonetheless, transgenic mouse lines that offer relatively faithful reproductions of a subset of AD features can help decipher the complexity of the disease and substantially contribute to diagnostic and therapeutic innovations⁶². In most mouse models, AD is triggered by the overexpression of APP mutant that cause familial AD in human. In the present study, APPsw tg mice expressed the human APP695 Swedish mutant under the control of the NSE promoter⁵⁵. These mice rarely exhibited A β plaques and concophilic deposits, and did not express NFT that consists of hyperphosphorylated tau at 12months. On the other hand, we observed more intraneuronal A β accumulation and greater phosphorylated tau levels in APPsw tg mice than in age matched wild mice, and APPsw tg mice showed cognitive impairment at 12months. These data suggest that APP tg mice as an AD animal model do not absolutely mimic the pathological conditions of AD, but investigations

using these mice are valid for evaluating the therapeutic potential of hNSCs, because intracellular amyloid leads to more progressive neuronal degeneration and death than extracellular A β burden, and the increase of phosphorylated tau is also detected in early AD^{55,62,63}. Intracerebroventricular transplanted hNSCs robustly migrate throughout the brains of APPsw tg mouse; they subsequently engraft to the SVZ, corpus callosum, fornix, thalamus, septofimbrial nuclei, cigulu, striatum, and cortex, although they are rarely detected in the hippocampal region. Although BrdU labeling and naive cells are widely through mouse brains, GFP-expressing hNSCs are difficult to observe due to the down-regulation of GFP⁸². Most hNSCs remain immature and an un-committed state; a few cells differentiate into immature neurons, astrocytes and oligodendro progenitors. It is thought that xenografts of hNSCs restrict the potential of multiple lineages, due to difference from the environment and in the time scale required for differentiation between humans and rodents⁸³. Human NSCs in APPsw tg mice still expressed A β degradase in the present study, and other previous studies report functional secretion of disease-modified factors in mouse brains transplanted with hNSCs. Therefore, hNSCs observed in APPsw tg mice are not quiescent and can interact with host cells, and never form tumors⁸⁴ in the brain of all transplanted mice. Human NSC grafts into the brains of APPsw tg mice improved the spatial memory, motor learning, and female forelimb strength, but not circadian, emotional, and locomotorial activity. Additionally, these behavioral tests were concomitantly conducted with either hNSC grafted or H-H buffer injected age matched wild mice. Interestingly, hNSC transplantation in the brains of wild mice had no change of cognition. It is thought that intracerebroventricular hNSC injections in wild mice did not result in "younger" behavior per se because age-related cognitive impairments do not result from a profound loss of neurons⁸⁵ but is mainly mediated by synaptic alterations in otherwise intact circuits^{85,86}. Next, we investigated how hNSCs ameliorate the behavior in APPsw tg mice compared to H-H buffer injected mice with respect to the vulnerable environment of AD brains. A β is continuously generated, and its concentration is partially determined by the activities of several degradative enzymes including NEP, IDE, ECE-1/2, MMP2/3/9, plasminogen

activators, and CTSB⁶⁴⁻⁶⁶. Decreased activity of these enzymes due to genetic mutations, age- or disease-related alterations in gene expression, or proteolytic activity, may increase the risk of AD⁶⁴. Thus, researchers apply these enzyme-expressing viral vectors and fibroblasts in AD animal models. As a result of these studies, these mice exhibited decreases of A β levels and burdens, and improvement of cognition⁸⁷⁻⁸⁹. In our study, hNSC grafting decreased intracellular A β 42 deposits in the cortex and hippocampus of APPsw tg mouse, and reduced soluble A β 42 levels in brains of APPsw tg mice. Human NSCs produced A β degradases, and especially human CTSB, IDE, ECE1, PLAT and PLAU were still detected in hNSC grafted mice. Therefore, hNSCs primarily degrade A β 42 in the ventricles where they are transplanted and secondarily regulate A β 42 levels to multiple regions engrafted because these enzymes have both a membrane bound and a diffusible secreted form, although engraftment was not observed in the hippocampus of hNSC grafted mice. There were no changes in soluble and insoluble A β 40 levels, because the strong expression of CTSB preferentially degrades A β 42 to A β 40⁶⁶. It is thought that the reduction of soluble A β 42 improves the spatial memory of hNSC grafted APPsw tg mice. Furthermore, hNSCs reduced the levels of phosphorylated tau. Previous studies found that NSC administration in the hippocampus increased the expression of endogenous BDNF in 3XTG mice⁴⁸, and that BDNF dephosphorylated tau via PI3k/Akt and GSK3 β signaling⁶⁹ and enhances motor skill acquisition⁹⁰. GSK3 β is one of the main tau kinases; it modifies several sites of the tau protein present in the NFT⁶⁸. The alteration of endogenous BDNF in hNSC grafted mice compared to H-H buffer grafted mice is not estimated, nonetheless, hNSC transplantation in APPsw tg mice is able to induce endogenous BDNF⁴⁸. Moreover, in vitro, hNSCs expressed various neurotrophins including BDNF. Neurotrophins secreted from hNSCs inhibit the activation of GSK3 β via the Trk-mediated phosphorylation of Akt⁶⁹; thus, the phosphorylation of tau in APPsw tg mice is reduced by hNSC. This signal transduction pathway is also operated by VEGF and GDNF secreted from hNSCs because VEGF and GDNF receptors are tyrosin kinase receptors^{91,92}. The trophic and growth factors generated from hNSCs enhanced motor learning in hNSC grafted

APPsw tg mice, which is consistent with a previous report⁹⁰. These factors can modify the degenerative conditions of the brains of APPsw tg mice. According to the regenerative and protective effects of NSCs, their transplantation increases the synaptic density in the CA1 striatum radiatum of APPsw tg mice and decreases apoptosis via these. These data support the idea that hNSC grafting prevents neuronal loss and enhances synaptic transmission in APPsw tg mice. Thus hNSC grafted APPsw tg mice have improved spatial memory compared to H-H buffer injected mice. Astrocytes and microglia become chronically activated in AD, contributing to and reinforcing the inflammatory cascade^{28,70,71}. APPsw tg mouse relatively signifies more inflammatory conditions than age matched wild mice⁵⁵. The transplantation of hNSCs in APPsw tg mice attenuated and modulated neuroinflammation. The number of microglia was decreased and their morphology was closer to the inactive form, especially in the motor cortex observing the robust engrafting of hNSCs as a additional evidence of improved motor learning. Astrogliosis and microgliosis were significantly decreased in the hippocampus of hNSC grafted APPsw tg mice. Therefore, it is thought that the suppression of inflammation increases the cognitive function of APPsw tg mice. Surprisingly, hNSCs expressed IL1ra, IL10, IL4 and TGF β when exposed to pro-inflammatory cytokines in vitro. NSCs can produce cytokines and chemokines in animal models of neurological disorders and attenuate neuroinflammation^{46,47}. Consistent with previous reports, intracerebroventricular hNSCs secrete anti-inflammatory cytokines, which lessen neuroinflammation. On the other hand, other studies assert that activated microglia have a beneficial effect via the phagocytosis of A β plaques in AD animal models⁹³⁻⁹⁵. It is currently known that extracellular A β plaques do not directly occur in the disease-related impairment in AD animal models and patients^{10,61}. Therefore active microglia can develop more vulnerable and degenerative environment in AD even though these phagocytose A β burden^{28,70,71}. In our study, the administration of hNSCs, which diminish A β 42 toxicity and secrete anti-inflammatory cytokines, resulted in weakened inflammation in APPsw tg mice. At the 3month-follow up in hNSC grafted APPsw tg mice, cognitive improvement was not significantly maintained, although learning and memory function

were slightly refined. Several factors generated from hNSCs do not inhibit progressive cognitive impairment for a long time. However, hNSCs can be genetically modified to express specific factors that change the AD environment or repeated hNSC injection can sustain positive effects for a long period of time.

In summary, our findings demonstrate that hNSC grafting in the AD-like animal model efficiently restores spatial memory, motor learning, and female forelimb strength without side effects. These are the result of the modified environment of the brains of APP^{sw} tg mice due to several factors generated from hNSCs. However, it is difficult to look forward to replacing lost cells in mice, because most hNSCs stay in an immature state. We conclude that hNSC based therapy has potential mainly by modifying the degenerative condition of mice by focusing on A β toxicity, tau instability, and neuroinflammation.

V. CONCLUSION

The transplantation of stem cells or their derivatives, as well as the activation of endogenous stem cells within the adult brain, are proposed as future therapies for neurodegenerative diseases, especially AD. However, it may seem unrealistic to induce functional recovery by replacing lost cells and protecting existing ones in AD brains considering the complexity of the structure and function of the human brain. Nevertheless, studies using animal models for other neurological disorders demonstrate that neuronal replacement and partial reconstruction of damaged neuronal circuitry is possible. There is also evidence from clinical trials that cell replacement in diseased human brains can lead to symptomatic relief.

In the present study, lenti-APPsw_GFP infected SK-N-MC cells generated naturally secreted A β oligomers. The AD animal model utilized mice that express the human APPsw mutant (KM595/596NL), which is directed by the NSE promoter. Human NSCs were isolated from human fetal telencephalon at 13 weeks of gestation; the procedure was approved by the ethics committee of Yonsei University College of Medicine. The naturally secreted A β oligomers affect the proliferation and differentiation of hNSCs in vitro, and hNSCs transplanted into the LVs of APPsw tg mice engraft, migrate, differentiate, and interact in the host brain. When conditioned media including the naturally secreted A β oligomers were directly treated, the proliferation of hNSCs was down-regulated, because A β oligomers induced senescence and not cell death. Exposure to the naturally secreted A β oligomers also led to gliogenesis of the hNSCs with respect to the expression levels of proteins and mRNAs. Human NSCs that were implanted into the LVs of 13month-old APPsw tg mice survived, migrated, and integrated into the corpus callosum, fornix, thalamus, septofimbrial nuclei, cingulum, striatum, and cortex. Engrafted hNSCs were mostly maintained as immature progenitors and partially differentiated into neurons, astrocytes, or oligodendrocytes. The transplantation of hNSCs ameliorated the pathological hallmarks of AD. Soluble A β 42 and phosphorylated tau levels decreased in the cortex and hippocampus due to distinct A β degradases and neurotrophins produced by the

hNSCs. In the vulnerable environment of the brains of APPsw tg mice, hNSCs also exhibited a neuroprotective effect via the secretion of trophic factors and anti-inflammatory cytokines. Lastly, hNSC grafting improved the spatial memory, motor learning, and female forelimb strength without side effects compared to H-H buffer grafted into the LVs of APPsw tg mice, although the amelioration was not maintained for a long time. For several years, most experts predicted that NSCs could be reliably used to replace damaged cells and tissues in the CNS. Barring cell replacement, NSCs are also known to lead to improvements via the secretion of biochemicals that engender improved neuronal function, promote survival, decrease inflammation, and encourage the growth of blood vessels. Nevertheless, investigations of the therapeutic potential of NSCs in AD are rarely reported because it is difficult to study this disease due to widespread and progressive pathological change. In this study, donor-derived hNSCs were widely distributed in the brain of APPsw tg mice, but cell replacement is rarely expected because the majority of engrafted hNSCs retain immature properties. Instead, hNSCs produce A β degradases, trophic factors, and anti-inflammatory cytokines, which reciprocally ameliorate AD-like symptoms in APPsw tg mice. In future studies, we will genetically modify hNSCs to express beneficial factors, including A β degradases, neurotrophic factors, growth factors, and anti-inflammatory cytokines, using transient or long-term expressing viral vectors. In addition, we will screen for factors of hNSCs related to their survival and functioning in mice as well as induce specific neural cell types to replace lost cells, such as in stem cell therapy for Parkinson's disease. We will confirm whether our findings are reproducible when hNSCs are transplanted in other APP animal models. Above all, among the spatial, temporal and methodological changes of hNSC administration, we will optimize an hNSC based therapy for clinical trials. We suggest that an hNSC based therapy could be an invaluable strategy for overcoming the limited treatments for AD.

REFERENCES

1. Hebert LE, Scherr PA, Bienias JL, Bennett DA, Evans DA. Alzheimer disease in the US population : Prevalence estimates using the 2000 census. *Arch Neurol* 2002;60:1119-22
2. Dubois B, Feldman HH, Jacova C, Dekosky ST, Barberger-Gateau P, Cummings J, et al. Research criteria for the diagnosis of Alzheimer's disease: revising the NINCDS-ADRDA criteria. *Lancet Neurol*. 2007;6:734-46
3. Alzheimer Association. 2010 Alzheimer's disease facts and figures. *Alzheimers Dement*. 2010;6:158-94
4. Selkoe DJ. The molecular pathology of Alzheimer's disease. *Neuron*. 1991;6:487-98
5. Ballatore C, Lee VM, Trojanowski JQ. Tau-mediated neurodegeneration in Alzheimer's disease and related disorders. *Nat Rev Neurosci*. 2007;8:377-91
6. Pearson RCA, Esiri MM, Hiorns RW, Wilcock GK, Powell TPS. Anatomical correlates of the distribution of the pathological changes in the neocortex in Alzheimer disease. *Proc. Natl. Acad. Sci. USA*. 1985;82:4531-4
7. Selkoe DJ. Normal and abnormal biology of the β -amyloid precursor protein. *Annu Rev Neurosci* 1994;17:489-517.
8. Hardy J, Selkoe DJ. The amyloid hypothesis of Alzheimer's disease: Progress and problems on the road to therapeutics. *Science* 2002;297:353-6
9. Yankner BA, Lu T. Amyloid β -protein toxicity and the pathogenesis of Alzheimer Disease. *J. Biol. Chem*. 2009;284:4755-9
10. Walsh DM, Selkoe DJ. A β oligomers - a decade of discovery. *J. Neurochem*. 2007;101: 1172-84
11. Haass C, Selkoe DJ. Soluble protein oligomers in neurodegeneration: lessons from the Alzheimer's amyloid β -peptide. *Nat. Rev. Cell. Biol*. 2007;8:101-12
12. Medeiros R, Baglietto-Vargas D, LaFerla FM. The role of tau in Alzheimer's disease and related disorders. *CNS neurosci Ther*. 2010; in press
13. Querfurth HW, LaFerla FM. Alzheimer's disease. *N. Engl. J. Med*. 2010;362:329-44

14. Mark P, Mattson. Pathways towards and away from Alzheimer's disease. *Nature* 2004;430: 631-9.
15. Tanzi RE, Bertram L. Twenty years of the Alzheimer's disease amyloid hypothesis: A genetic perspective. *Cell* 2005;120:545-55.
16. Selkoe DJ, Wolfe MS. Presenilin:running with scissors in the membrane. *Cell*. 2007;131: 215-21
17. Kounnas MZ, Danks AM, Cheng S, Tyree C, Ackerman E, Zhang X et al. Modulation of γ -secretase reduces β -amyloid deposition in a transgenic mouse model of Alzheimer's disease. *Neuron*. 2010;67:769-80
18. Bertram L, Lange C, Mullin K, Parkinson M, Hsiao M, Hogan MF et al. Genome-wide association analysis reveals putative Alzheimer's disease susceptibility loci in addition to APOE. *Am. J. Hum. Genet.* 2008;83:623-32
19. Dodart JC, Marr RA, Koistinaho M, Gregersen BM, Malkani S, Verma IM, et al. Gene delivery of human apolipoprotein E alters brain A β burden in a mouse model of Alzheimer's disease. *Proc. Natl. Acad. Sci. USA* 2005;102:1211-6.
20. Kim j, Basak JM, Holtzman DM. The role of apolipoprotein E in Alzheimer's disease. *Neuron* 2009;63:287-303
21. Weiner HL, Frenkel D. Immunology and immunotherapy of Alzheimer's disease. *Nat. Rev. Immunol.* 2006;6:404-16
22. Orgogozo JM, Gilman S, Dartigues JF, Laurent B, Puel M, Kirby LC et al. Subacute meningoencephalitis in a subset of patients with AD after abeta42 immunization. *Neurology*. 2003;61:46-54.
23. Pfeifer M, Boncristiano S, Bondolfi L, Stalder A, Deller T, Staufenbiel M et al. Cerebral hemorrhage after passive anti-Abeta immunotherapy. *Science*. 2002;298:1379
24. Lleó A, Greenberg SM, Growdon JH. Current pharmacotherapy for Alzheimer's disease. *Annu Rev Med* 2006;57:7.1-21.
25. Winkler J, Thal LJ, Gage FH, Fisher LJ. Cholinergic strategies for Alzheimer's disease. *J Mol Med* 1998;76:555-67.
26. Kar S, Slowikowski SPM, Westaway D, Mount HTJ. Interactions between β -amyloid and central cholinergic neurons : implication for Alzheimer's disease. *J Psychiatry Neurosci.* 2004;29: 427-41.

27. Huang X, Moir RD, Tanzi RE, Bush AI, Rogers JT. Redox-active metals, oxidative stress, and Alzheimer's disease pathology. *Ann NY Acad Sci* 2004;1012:153-163
28. Wyss-Coray T. Inflammation in Alzheimer disease: driving force, bystander or beneficial response? *Nat Med.* 2006;12:1005-15
29. Yan Q, Zhang J, Liu H, Babu-Khan S, Vassar R, Biere AL et al. Anti-inflammatory drug therapy alters β -amyloid processing and deposition in an animal model of Alzheimer's disease. *J. Neurosci.* 2003;23:7504-9
30. Conti L, Cattaneo E. Neural stem cell systems : physiological players or in vitro entities? *Nat. Rev. Neurosci.* 2010;11:176-87
31. McKay R. Stem cells in the central nervous system. *Science* 1997; 276:66-71.
32. Gage FH. Mammalian neural stem cells. *Science* 2000;287:1433-8.
33. Eriksson PS, Perfilieva E, Eriksson TB, Alborn AM, Nordborg C, Peterson DA, Gage FH. Neurogenesis in the adult human hippocampus. *Nat Med* 1998;4:1313-7
34. Ming GI, Song H. Adult neurogenesis in the mammalian central nervous system. *Annu Rev Neurosci.* 2005;28:223-50
35. Kriegstein A, Alvarez-Buylla A. The glial nature of embryonic and adult neural stem cells. *Annu. Rev. Neurosci.* 2009;32:149-84
36. Suh H, Deng W, Gage FH. Signaling in adult neurogenesis. *Annu. Rev. Cell. Dev. Biol.* 2009;25:253-75
37. Svendsen CN, ter Borg MG, Armstrong RJ, Rosser AE, Chandran S, Ostenfeld T, Caldwell MA. A new method for the rapid and long term growth of human neural precursor cells. *J Neurosci Methods.* 1998;85:141-53.
38. Vescovi AL, Parati EA, Gritti A, Poulin P, Ferrario M, Wanke E et al. Isolation and cloning of multipotential stem cells from the embryonic human CNS and establishment of transplantable human neural stem cell lines by epigenetic stimulation. *Exp Neurol.* 1999;156:71-83.
39. Reynolds BA, Weiss S. Generation of neurons and astrocytes from isolated cells of the adult mammalian central nervous system. *Science.* 1992;255:1707-10.
40. Palmer TD, Ray J, Gage FH. FGF-2 responsive neuronal progenitors reside in proliferative and quiescent regions of the adult rodent brain. *Mol Cell Neurosci* 1995;6:474-86

41. Park KI, Teng YD, Snyder EY. The injured brain interacts reciprocally with neural stem cells supported by scaffolds to reconstitute lost tissue. *Nat Biotechnol* 2002;20:1111-7.
42. Kelly S, Bliss TM, Shah AK, Sun GH, Ma M, Foo WC et al. Transplanted human fetal neural stem cells survive, migrate, and differentiate in ischemic rat cerebral cortex. *Proc Natl Acad Sci U S A*. 2004;101:11839-44.
43. Abematsu M, Tsujimura K, Yamano M, Saito M, Kohno K, Kohyama J et al. Neurons derived from transplanted neural stem cells restore disrupted neuronal circuitry in a mouse model of spinal cord injury. *J. Clin. Invest.* 2010;120:3255-66
44. Lee JP, Jeyakumar M, Gonzalez R, Takahashi H, Lee P, Baek RC et al. Stem cells act through multiple mechanisms to benefit mice with neurodegenerative metabolic disease. *Nat. Med.* 2007;13:439-47
45. Tamaki SJ, Jacobs Y, Dohse M, Capela A, Cooper JD, Reittsma M et al. Neuroprotection of host cells by human central nervous system stem cells in a mouse model of infantile neuronal ceroid lipofuscinosis. *Cell Stem cell.* 2009;5:310-19
46. Pluchino S, Zanotti L, Rossi B, Brambilla E, Ottoboni L, Salani G et al. Neurosphere-derived multipotent precursors promote neuroprotection by an immunomodulatory mechanism. *Nature.* 2005;436:266-71
47. Martino G, Pluchino S. The therapeutic potential of neural stem cells. *Nat. Rev. Neurosci.* 2006;7:395-406
48. Blurton-Jones M, Kitazawa M, Martinez-Coria H, Castello NA, Muller F, Loring JF et al. Neural stem cells improve cognition via BDNF in a transgenic model of Alzheimer's disease. *Proc Natl Acad Sci U S A*. 2009;106:13594-9
49. Marutle A, Ohmitsu M, Nilbratt M, Greig NH, Nordberg A, Sugaya K. Modulation of human neural stem cell differentiation in Alzheimer (APP23) transgenic mice by phenserine. *Proc Natl Acad Sci U S A*. 2007;104:12506-11.
50. Jakel RJ, Schneider BL, Svendsen CN. Using human neural stem cells to model neurological disease. *Nat Rev Genet.* 2004;5:136-44.
51. Goldman S. Stem and progenitor cell based therapy of the human central nervous system. *Nat Biotechnol* 2005;7:862-71
52. Lindvall O, Kokaia Z. Stem cells in human neurodegenerative disorders - time for clinical translation? *J Clin Invest.* 2010;120:29-40

53. Kim HT, Kim IS, Lee IS, Lee JP, Snyder EY, Park KI. Human neurospheres derived from the fetal central nervous system are regionally and temporally specified but are not committed. *Exp. Neurol.* 2006;199:222-35
54. Mullan M, Crawford F, Axelman K, Houlden H, Lilius L, Winblad B et al. A pathogenic mutation for probable Alzheimer's disease in the APP gene at the N-terminus of β -amyloid. *Nat Genet* 1992;1:345-7
55. Hwang DY, Cho JS, Lee SH, Chae KR, Lim HJ, Min SH, et al. Aberrant expression of pathogenic phenotype in Alzheimer's diseased transgenic mice carrying NSE-controlled APPsw. *Exp Neurol* 2004;186:20-32.
56. Walsh DM, Klyubin I, Fadeeva JV, Cullen WK, Anwyl R, Wolfe MS et al. Naturally secreted oligomer of amyloid β protein potently inhibit hippocampal long-term potentiation in vivo. *Nature.* 2002;416:535-9
57. Cleary JP, Walsh DM, Hofmeister JJ, Shankar GM, Kuskowski MA, Selkoe DJ et al. Natural oligomers of the amyloid- β protein specifically disrupt cognitive function. *Nat Neurosci.* 2004;8:79-84
58. Klyubin I, Walsh DM, Lemere CA, Cullen WK, Shankar GM, Betts V et al. Amyloid β protein immunotherapy neutralizes A β oligomers that disrupt synaptic plasticity in vivo. *Nat Med.* 2005;11:556-61
59. Podlisny MB, Ostaszewski BL, Squazzo SL, Koo EH, Rydell RE, Teplow DB et al. Aggregation of secreted amyloid β -protein into sodium dodecyl sulfate-stable oligomers in cell culture. *J. Biol. Chem.* 1995;270:9564-70
60. Shankar GM, Li S, Mehta TH, Gracia-Munoz A, Shepardson NE, Smith I et al. Amyloid- β protein dimers isolated directly from Alzheimer's disease impair synaptic plasticity and memory. *Nat Med.* 2008;14:837-42
61. Hardy J. The amyloid hypothesis for Alzheimer's disease : a critical reappraisal. *J Neurochem* 2010;110:1129-34
62. McGowan E, Eriksen J, Hutton M. A decade of modeling Alzheimer's disease in transgenic mice. *Trends Genet.* 2006;22:281-9
63. LaFerla FM, Green KN, Oddo S. Intracellular amyloid- β in Alzheimer's disease. *Nat Rev Neurosci.* 2007;8:499-509
64. Nalivaeva NN, Fisk LR, Belyaev ND, Turner AJ. Amyloid degrading enzymes as therapeutic targets in Alzheimer's disease. *Curr Alzheimer Res.* 2008;5:212-24

65. Turner AJ, Nalivaeva. New insights into the roles of metalloproteinases in neurodegeneration and neuroprotection. *Int. Rev. Neurobiol.* 2007;82:113-34
66. Mueller-Steiner S, Zhou Y, Arai H, Roberson ED, Sun B, Chen J et al. Antiamyloidogenic and neuroprotective functions of cathepsin B : implications for Alzheimer's disease. *Neuron* 2006; 51:703-14
67. Noble W, Planel E, Zehr C, Olm V, Meyerson J, Suleman F et al. Inhibition of glycogen synthase kinase-3 by lithium correlates with reduced tauopathy and degeneration in vivo. *Proc Natl Acad Sci U S A.* 2005;102:6990-5
68. Avila J, Wandosell F, Hernandez F. Role of glycogen synthase kinase-3 in Alzheimer's disease pathogenesis and glycogen synthase kinase-3 inhibitors. *Expert Rev Neurother.* 2010;10: 703-10
69. Elliott E, Atlas R, Lange A, Ginzburg I. Brain-derived neurotrophic factor induces a rapid dephosphorylation of tau protein through a PI-3kinase signalling mechanism. *Eur J Neurosci.* 2005;22:1081-9
70. Heneka MT, O'Banion MK, Terwel D, Kummer MP. Neuroinflammatory processes in Alzheimer's disease. *J Neural Transm.* 2010;117:919-47
71. Hohlfeld R, Kerschensteiner M, Meinel E. Dual role of inflammation in CNS disease. *Neurology.* 2007;68:S58-63
72. Dickson DW. Apoptotic mechanisms in Alzheimer neurofibrillary degeneration : cause or effect? *J Clin Invest* 2004;114:23-7
73. Nagahara AH, Merrill DA, Coppola G, Tsukada S, Schroeder BE, Shaked GM et al. Neuroprotective effects of brain-derived neurotrophic factor in rodent and primate models of Alzheimer's disease. *Nat Med.* 2009;15:331-7
74. Park S, Kim HT, Yun S, Kim IS, Lee J, Lee IS et al. Growth factor-expressing human neural progenitor cell grafts protect motor neurons but do not ameliorate motor performance and survival in ALS mice. *Exp Mol Med.* 2009;41:487-500
75. Lopez-Toledano MA, Shelanski ML. Neurogenic effect of β -amyloid peptide in the development of neural stem cells. *J Neurosci.* 2004;24:5439-44
76. Uchida Y, Nakano SI, Gomi F, Takahashi H. Differential regulation of basic helix-loop-helix factors mash1 and olig2 by β -amyloid accelerates both differentiation and death of cultured neural stem/progenitor cells. *J Biol Chem.* 2007;282:1970-9

77. Millet P, Lages CS, Haik S, Nowak E, Allemand I, Granotier C et al. Amyloid- β peptide triggers Fas-independent apoptosis and differentiation of neural progenitor cells. *Neurobiol Dis.* 2005;19:57-65
78. Heo C, Chang KA, Choi HS, Kim HS, Kim S, Liew H et al. Effects of the monomeric, oligomeric, and fibrillar A β 42 peptides on the proliferation and differentiation of adult neural stem cells from subventricular zone. *J Neurochem.* 2007;102:493-500
79. Eucher JN, Uemura E, Sakaguchi DS, West Greenlee MH, Amyloid-beta peptide affects viability but not differentiation of embryonic and adult rat hippocampal progenitor cells. *Exp Neurol.* 2007;203:486-92
80. He P, Shen Y. Interruption of β -catenin signaling reduces neurogenesis in Alzheimer's disease. *J Neurosci.* 2009;29:6545-57
81. Haughey NJ, Nath A, Chan SL, Borchard AC, Rao MS, Mattson MP. Disruption of neurogenesis by amyloid β -peptide, and perturbed neural progenitor cell homeostasis, in models of Alzheimer's disease. *J Neurochem.* 2002;83:1509-24
82. Guillaume DJ, Johnson MA, Li XJ, Zhang SC. Human embryonic stem cell-derived neural precursors develop into neurons and integrate into the host brain. *J Neurosci Res.* 2006;84: 1165-76
83. Suzuki M, Svendsen CN. Combining growth factors and stem cell therapy for amyotrophic lateral sclerosis. *Trends Neurosci.* 2008;31:192-8
84. Jandial R, Snyder EY. On guard against cancer. *Nat Med.* 2009;15:999-1001
85. Hof PR, Morrison JH. The aging brain : morphomolecular senescence of cortical circuits. *Trends Neurosci.* 2004;27:607-13
86. Burke SN, Barnes CA. Neural plasticity in the ageing brain. *Nat Rev Neurosci.* 2006;7:30-40
87. Hemming ML, Patterson M, Reske-Nielsen C, Lin L, Isacson O, Selkoe DJ. Reducing amyloid plaque burden via ex vivo gene delivery of an A β -degrading protease: a novel therapeutic approach to Alzheimer disease. *PLoS Med.* 2007;4: 1405-16.
88. Carty NC, Nash K, Lee D, Mercer M, Gottschall PE, Meyers C et al. Adeno-associated viral (AAV) serotype 5 vector mediated gene delivery of endothelin-

converting enzyme reduces A β deposits in APP+PS1 transgenic mice. *Mol Ther.* 2008;16:1580-6

89. Leissring MA, Farris W, Chang AY, Walsh DM, Wu X, Sun X et al. Enhanced proteolysis of β -amyloid in APP transgenic mice prevents plaque formation, secondary pathology, and premature death. *Neuron.*2003;40:1087-93

90. Fritsch B, Reis J, Martinowich K, Schambra HM, Ji YY, Cohen LG et al. Direct current stimulation promotes BDNF-dependent synaptic plasticity : potential implications for motor learning. *Neuron.* 2010;66:198-204

91. Ferrara N, Gerber HP, LeCouter J. The biology of VEGF and its receptors. *Nat Med.* 2003; 9:669-76

92. Airaksinen MS, Saarma M. The GDNF family : signalling, biological functions and therapeutic value. *Nat Rev Neurosci.* 2002;3:383-94

93. Simard AR, Soulet D, Gowing G, Julein JP, Rivest S. Bone marrow-derived microglia play a critical role in restricting senile plaque formation in Alzheimer's disease. *Neuron.* 2006;49:489-502

94. Khoury JE, Toft M, Hickman SE, Means TK, Terada K, Geula C. Ccr2 deficiency impairs microglial accumulation and accelerates progression of Alzheimer-like disease. *Nat Med.* 2007;13: 432-8

95. Lee JK, Jin HK, Endo S, Schuchman EH, Carter JE, Bae JS. Intracerebral transplantation of bone marrow-derived mesenchymal stem cells reduces amyloid-beta deposition and rescues memory deficits in Alzheimer's disease mice by modulation of immune response. *Stem Cells.* 2010;28:329-43

ABSTRACT(IN KOREAN)

알츠하이머질환 모델에서 인간 신경줄기세포 뇌 이식의 치료 유용성

<지도교수 박국인>

연세대학교 대학원 의과학과

이 일 신

알츠하이머병은 전 세계적으로 삼천 오백 만 명 이상의 환자가 이환되어 있는 대표적인 만성 진행성 노인성 치매 질환인데, 환자는 주로 기억력, 사고력, 지남력, 이해력, 계산능력, 학습능력, 언어 및 판단력 등에 있어서 다발성으로 뇌 기능 장애를 보인다. 알츠하이머병 환자의 뇌에서 관찰되는 특징적인 병리조직학적 소견은 전반적인 뇌 위축 (diffuse brain atrophy), 뇌실확장 (cerebral ventricular dilatation), 뇌신경세포 내 신경섬유의 다발성 병변 (neurofibrillary tangle) 및 신경세포외 공간 (extracellular space)에 초로성 반점 (senile plaque) 형성 등을 들 수 있다.

신경줄기세포는 발달단계의 신경계뿐만 아니라 성체 중추신경계에서도 존재하며, 자가갱신 (self-renewal)하고 다양한 신경세포로 분화할 수 있는 분화의 다능성 (multipotency)을 보이는 미성숙 신경세포이다. 본 세포는 시험관 내에서 증식되어 생체 내 이식이 가능하며, 이식 된 세포는 숙주 신경계의 전체 신경축 (neuraxis)에 걸쳐 광범위하게 이주, 생착, 통합되어 치료적으로 유용한 물질을 직접적, 지속적, 그리고 조절되는 양상으로 분비할 수 있다. 또 급만성 퇴행성 신경병소 유래 미세환경신호에 반응하여 신경병소 부위로 특이적으로 이주하고, 세포 구조학적 및 기능적으로 적절한 신경세포로 분화함을 보여 난치성 신경계질환에서 치료적 유용성을 보인다.

본 연구는 알츠하이머병에서 인간 신경줄기세포 이식의 치료적 유용성을 조사하였는데, 동물모델로서 인간 APP (amyloid precursor protein) 유전자의 670번 amino acid가 Lys에서 Asp으로, 671번 Met이 Leu으로 변이된 APP^{swe} (APP swedish mutation) 형질전환 쥐를 사용하였고, 렌티바이러스를 이용 soluble A β oligomer를 지속적으로 분비케 한 SK-N-MC 세포주를 확립하여 인간 신경줄기세포의 증식, 성장 및 분화에 미치는 영향을 분석하였다. 인간 신경줄기세포는 임신 13주에 자연 유산된 태아의 중뇌에서 분리, 배양하였다.

Soluble A β oligomer가 인간 신경줄기세포의 성장과 분화에 미치는 영향을 조사하였는데, 시험관 내에서 SK-N-MC 세포에서 분비된 soluble A β oligomer는 신경줄기세포의 노화를 유도하여 세포증식을 감소시키고 주로 신경교세포로의 분화를 유도하였다. 알츠하이머병 모델에서 인간 신경줄기세포 뇌 이식의 치료적 유용성을 평가하기 위하여 생후 13개월 된 APP^{swe} 형질전환 쥐의 측 내실에 세포를 이식하고 8주 후에 분석한 결과, 공여세포는 모델동물 뇌의 다양한 부위에 걸쳐 광범위하게 이주 및 정착함을 보였고, 일부 공여세포는 신경원세포, 희소돌기아교세포 및 성상세포로 분화하였지만 대부분의 공여세포는 주로 미분화 상태로 존재하였다. 모델동물에서 인간 신경줄기세포를 뇌 이식한 실험군과 식염수를 주사한 대조군에서 신경행동검사를 실시하였는데, 실험군에서 줄기세포 이식에 따른 비정상적 신경기능 및 행동이 관찰되지 않았고 대조군에 비해 실험군에서 모델동물의 공간 기억능력 및 운동 학습능력이 향상됨을 보였다.

알츠하이머병 모델에서 인간 신경줄기세포 뇌 이식이 신경행동학적 기능향상을 유도하는 기전으로, 첫째 인간 신경줄기세포는 다양한 종류의 A β (amyloid beta protein) degradase를 분비하여 숙주동물 뇌의 신경세포 내 A β 42의 농도를 감소시켰으며 둘째, 인간 신경줄기세포는 다양한 종류의 신경영양인자들을 분비하여 PI3K/Akt signaling을 활성화 시키고 tau의 인산화를 억제함을 보였고 셋째, 인간 신경줄기세포는 다양한 항염증 사이토카인 등을 분비하여 실험군에서 뇌의 염증반응 (astrogliosis 및 microgliosis) 감소를 유도하였으며 넷째, 실험군에서는 대조군에 비해 신경세포의 시냅스 전 치밀도 (presynaptic density)가 증가함을 나타내 신경신호전달 기능이 향상됨을 보였고 다섯째, 공여세포에서 발현되는 다양한 신경영양인자들의 작용으로 인하여 실험군에서 대조군에 비해 신경세포 사멸이 감소함을 보였다.

이상으로 알츠하이머병 동물모델에서 인간 신경줄기세포 뇌 이식 시 공여세포는 숙주동물 뇌의 광범위한 부위에 이주, 정착 및 통합되고 미만성 및 비미만성 인자들을 발현하여 다양한 기전으로 알츠하이머병 특이 신경병리 환경을 변화시켜 숙주동물에서 학습 및 기억능력 등의 신경행동학적 기능이 개선됨을 보였고, 세포이식에 따른 특별한 부작용은 관찰되지 않았다. 따라서 현재까지 특별한 치료법이 없는 알츠하이머병에서 인간 신경줄기세포의 뇌 이식은 유용한 치료법으로 사용될 수 있음을 제시하였다.

핵심되는 말 : 알츠하이머병, 인간 신경줄기세포, APP 형질전환 쥐, 세포치료